

STATUS OF THESIS

Title of thesis

**A Study on an Evaporator-Condenser Combination for Humidity Control in an Air-Conditioning System**

I

**CHAN KAR FYE**  
(CAPITAL LETTERS)

hereby allow my thesis to be placed at the Information Resource Center (IRC) of Universiti Teknologi PETRONAS (UTP) with the following conditions:

1. The thesis becomes the property of UTP
2. The IRC of UTP may make copies of the thesis for academic purposes only.
3. This thesis is classified as

Confidential

Non-confidential

If this thesis is confidential, please state the reason:

The principle and details of the evaporator-condenser system are being considered for a patent application. Therefore, any prior disclosure cannot be permitted. For this reason, the confidentiality is to be maintained for the required period.

The contents of the thesis will remain confidential for 5 years.

Remarks on disclosure:

N/A



Signature of Author  
Permanent address:

38, Pesara Wah Keong,  
Taman Wah Keong,  
31400 Ipoh.

Perak Darul Ridzuan

Date : 4/6/12

Endorsed by



Signature of Supervisor

Dr. Vijay R. Raghavan

Name of Supervisor

Date : 4/6/12

UNIVERSITI TEKNOLOGI PETRONAS

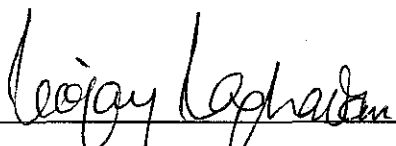
A STUDY ON AN EVAPORATOR-CONDENSER COMBINATION FOR  
HUMIDITY CONTROL IN AN AIR-CONDITIONING SYSTEM

by

CHAN KAR FYE

The undersigned certify that they have read, and recommend to the Postgraduate Studies Programme for acceptance this thesis for the fulfilment of the requirements for the degree stated.

Signature:

  
\_\_\_\_\_

Main Supervisor:

Dr. Vijay R. Raghavan  
\_\_\_\_\_

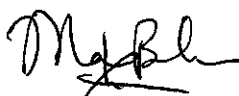
Signature:

  
\_\_\_\_\_

Co-Supervisor:

Assoc. Prof. Ir. Dr. Shaharin Anwar Sulaiman  
\_\_\_\_\_

Signature:

  
\_\_\_\_\_

Head of Department:

Ir. Dr. Masri Baharom  
\_\_\_\_\_

Date:

4/6/12  
\_\_\_\_\_

Ir. Dr. Masri Baharom  
Head of Department/Senior Lecturer  
Department of Mechanical Engineering  
Universiti Teknologi PETRONAS  
Bandar Seri Iskandar 31750 Tronoh  
Perak Darul Ridzuan, Malaysia

A STUDY ON AN EVAPORATOR-CONDENSER COMBINATION FOR  
HUMIDITY CONTROL IN AN AIR-CONDITIONING SYSTEM

by

CHAN KAR FYE

A Thesis

Submitted to the Postgraduate Studies Programme

as a Requirement for the Degree of

MASTER OF SCIENCE

MECHANICAL ENGINEERING DEPARTMENT

UNIVERSITI TEKNOLOGI PETRONAS

BANDAR SERI ISKANDAR,

PERAK

APRIL 2012

DECLARATION OF THESIS

Title of thesis

**A Study on an Evaporator-Condenser Combination for Humidity Control in an Air-Conditioning System**

I

**CHAN KAR FYE**  
(CAPITAL LETTERS)

hereby declare that the thesis is based on my original work except for quotations and citations which have been duly acknowledged. I also declare that it has not been previously or concurrently submitted for any other degree at UTP or other institutions.



Signature of Author

Permanent address:

38, Pesara Wah Keong,

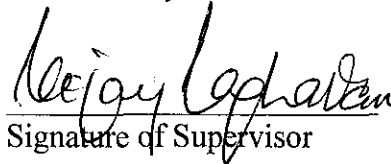
Taman Wah Keong,

31400 Ipoh.

Perak Darul Ridzuan

Date : 4/6/12

Witnessed by



Signature of Supervisor

Name of Supervisor

Prof. Dr. Vijay R. Raghavan

Date : 4/6/12

## ACKNOWLEDGEMENTS

During the course of this study, I have had the good fortune to meet friends who are not hesitant to provide assistance. It is due to a lot of people that this study could be completed.

First and foremost, I would like to thank my UTP post-graduate supervisor, Dr. Vijay R. Raghavan. Dr. Vijay has given me the opportunity to pursue my Post-graduate studies in UTP. His vast experience and knowledge has always been able to guide me in the right direction for this study.

I would also like to acknowledge my co-supervisor Assoc. Prof. Ir. Dr. Shararin Anwar Sulaiman for his invaluable advice during the course of this study.

My gratitude also goes to my field supervisor Dr. Chin Wai Meng and my industrial supervisor Mr. Thoo Kok Keong from O.Y.L. Research & Development Sdn. Bhd. They have always given me guidance in completing this study from an application point of view. Due to their experience working in the air conditioning field, I was able to experience the industrial environment that is expected of a research engineer.

Next, I would like to acknowledge O.Y.L. Research & Development Sdn. Bhd. for providing the funding and facilities for this study. It was the state of the art facilities and the know-how in the company that has paved the road for the completion of this study.

Finally, thanks to all the people who have helped me in any way, including the engineers and technicians of O.Y.L. Research & Development Sdn. Bhd. and friends and family who have always given encouragement and moral support.

## ABSTRACT

An experimental study has been performed on an evaporator-condenser system for humidity control using a constant speed compressor and fixed air volume. The evaporator-condenser system requires an addition of a reheat coil to the conventional unit. The reheat coil serves to reheat the cooled air leaving the cooling coils, thereby controlling the relative humidity. Preliminary simulations using the software Vapcyc and CoilDesigner show an improvement in the cooling performance and also an improvement in the dehumidification capability of the air conditioning system. Thereafter, an experimental study was performed using a modified commercial ceiling concealed air conditioning unit. Results from the experiments show that the dehumidification capability in terms of absolute humidity and relative humidity had improved, while the cooling performance had declined. Vapcyc and CoilDesigner are not suitable to simulate evaporator-condenser systems as they were only originally designed for conventional cooling systems. A comparison between the evaporator-condenser, desiccant wheel and loop heat pipe systems has been shown. While all systems are able to enhance moisture removal, the evaporator-condenser system is advantageous in simplicity, floor space and method of controlling the moisture removal rate. The concomitant benefits are a more comfortable environment, better productivity and more healthy conditions.

## ABSTRAK

Satu kajian telah dilakukan ke atas sistem penyejat-pemeluwap untuk kawalan kelembapan yang menggunakan pemampat kelajuan dan kadar aliran angin malar. Sistem penyejat-pemeluwap memerlukan penambahan gegelung pemanasan semula kepada unit konvensional. Gegelung pemanasan semula digunakan untuk memanaskan semula udara yang disejukan di gegelung penyejukan, dengan itu mengawal kelembapan. Simulasi awal menggunakan Vapcyc dan CoilDesigner menunjukkan peningkatan dalam prestasi penyejukan dan juga meningkatkan keupayaan penyahlembapan sistem penghawa dingin. Justeru itu, kajian menggunakan unit *ceiling conceal* komersial yang diubah suai. Keputusan daripada eksperimen menunjukkan bahawa keupayaan penyahlembapan dari segi kelembapan mutlak dan kelembapan telah meningkat, manakala prestasi penyejukan telah menurun. Vapcyc dan CoilDesigner tidak sesuai untuk mensimulasikan sistem penyejat-pemeluwap kerana mereka hanya direka bentuk untuk sistem penyejukan konvensional. Perbandingan antara system penyejat-pemeluwap, bahan pengering roda dan sistem gelung paip haba telah ditunjukkan. Walaupun semua sistem dapat meningkatkan pembuangan kelembapan, sistem penyejat-pemeluwap berfaedah dalam rekabentuk, ruang lantai dan kaedah mengawal kadar penyingkiran lembapan. Manfaat seiring persekitaran yang lebih selesa, produktiviti yang lebih baik dan suasana yang lebih sihat.

In compliance with the terms of the Copyright Act 1987 and the IP Policy of the university, the copyright of this thesis has been reassigned by the author to the legal entity of the university,

Institute of Technology PETRONAS Sdn Bhd.

Due acknowledgement shall always be made of the use of any material contained in, or derived from, this thesis.

© Chan Kar Fye, 2012  
Institute of Technology PETRONAS Sdn Bhd  
All rights reserved



## TABLE OF CONTENTS

| Chapter | Title  | Page |
|---------|--|------|
|         | Status of Thesis                             | i    |
|         | Approval Page                                | ii   |
|         | Title Page                                   | iii  |
|         | Declaration                                  | iv   |
|         | Dedication                                   | v    |
|         | Acknowledgements                             | vi   |
|         | Abstract                                     | vii  |
|         | Copyright Page                               | ix   |
|         | Table of Contents                            | x    |
|         | List of Tables                               | xiii |
|         | List of Figures                              | xiv  |
|         | List of Symbols, Abbreviations, Nomenclature | xvi  |
| 1.0     | INTRODUCTION                                 | 1    |
| 1.1     | Justification for the Research               | 3    |
| 1.2     | Objectives of Study                          | 4    |
| 1.3     | Scope of Study                               | 4    |
| 2.0     | LITERATURE REVIEW                            | 7    |
| 2.1     | Thermal Comfort                              | 7    |
| 2.1.1   | Thermal Comfort Index                        | 9    |
| 2.2     | Humidity Control                             | 9    |
| 2.2.1   | Dehumidifiers                                | 9    |
| 2.2.2   | Auxiliary Heater                             | 10   |
| 2.2.3   | Desiccant Wheel                              | 11   |
| 2.2.4   | Heat Pipe/Thermosyphon                       | 13   |
| 2.2.5   | Constant Speed Compressors                   | 14   |
| 2.2.6   | Variable Speed Compressors and Blowers       | 15   |
| 2.3     | Current Two-evaporator Applications          | 16   |
| 2.4     | Opportunities for Research                   | 19   |
| 2.5     | Chapter Summary                              | 22   |
| 3.0     | METHODOLOGY                                  | 23   |
| 3.1     | System Circuit Design                        | 23   |
| 3.2     | Vapcyc and CoilDesigner simulation           | 28   |
| 3.2.1   | Method                                       | 28   |
| 3.3     | Experimental Setup                           | 33   |
| 3.3.1   | Indoor Unit                                  | 33   |

|       |   |    |
|-------|---|----|
| 3.3.2 | Cooling Coil and Reheat Coil                  | 34 |
| 3.3.3 | Motor and Blower                              | 34 |
| 3.3.4 | Distributor                                   | 34 |
| 3.3.5 | Electronic Expansion Valve                    | 36 |
| 3.3.6 | Solenoid Valve                                | 37 |
| 3.3.7 | Check Valve                                   | 37 |
| 3.3.8 | Other Components                              | 39 |
| 3.4   | Measuring Equipment                           | 39 |
| 3.5   | Experimental Methodology                      | 42 |
| 3.5.1 | System Leak Check                             | 42 |
| 3.5.2 | Cooling System Refrigerant Optimization       | 42 |
| 3.5.3 | Humidity Control System Test                  | 44 |
| 3.5.4 | Measurement Uncertainty                       | 45 |
| 3.6   | Chapter Summary                               | 48 |
| 4.0   | RESULTS AND DISCUSSION                        | 49 |
| 4.1   | Implications of the Balancing Simulation      | 49 |
| 4.2   | Performance and Moisture Removal              | 51 |
| 4.3   | Coefficient of Performance                    | 54 |
| 4.4   | Relative Humidity                             | 56 |
| 4.5   | Comparing Simulation Results and Test Results | 58 |
| 4.5.1 | Refrigerant Mass Flow Rate                    | 59 |
| 4.5.2 | System Pressures                              | 61 |
| 4.6   | P-h Diagram Comparison                        | 62 |
| 4.7   | System Comparisons                            | 65 |
| 4.8   | Chapter Summary                               | 67 |
| 5.0   | CONCLUSIONS AND RECOMMENDATIONS               | 69 |
| 5.1   | Conclusions                                   | 69 |
| 5.2   | Recommendations                               | 70 |
|       | REFERENCES                                    | 71 |
|       | LIST OF PUBLICATIONS                          | 76 |

## APPENDICES

|   |  |    |
|---|--|----|
| A | Charge optimizing test data                        | 77 |
| B | Vapcyc balancing for YCC60c vs YSL61C              | 81 |
| C | Reheat coil test data                              | 82 |
| D | Refrigerant mass flow rate at different conditions | 83 |
| E | List of equations                                  | 84 |

## LIST OF TABLES

|           |   |    |
|-----------|---|----|
| Table 2.1 | Summary of common dehumidification methods            | 21 |
| Table 3.1 | Cooling coil and reheat coil specifications           | 34 |
| Table 3.2 | Performance at 80°C and 85°C discharge temperature    | 44 |
| Table 3.3 | List of uncertainties of measurement instruments      | 47 |
| Table 3.4 | Error propagation relationship                        | 47 |
| Table 4.1 | Simulation Results                                    | 50 |
| Table 4.2 | System performance of the evaporator-condenser system | 59 |

## LIST OF FIGURES

|             |  |    |
|-------------|--|----|
| Figure 1.1  | York ceiling concealed indoor unit YCC60C  | 5  |
| Figure 1.2  | York outdoor condensing unit YSL61C  | 5  |
| Figure 2.1  | Acceptable ranges of operative temperature and humidity based on a 10% dissatisfaction criteria for general (whole body) thermal comfort based on the PMV-PPD index, plus an additional 10% dissatisfaction that may occur on average from local (partial body) thermal discomfort | 8  |
| Figure 2.2  | Schematic of a dehumidifier  | 10 |
| Figure 2.3  | Relative humidity control by auxiliary heater  | 11 |
| Figure 2.4  | Schematic diagram of a desiccant wheel in an air-conditioning system   | 12 |
| Figure 2.5  | Schematic diagram of a heat pipe heat exchanger in an air conditioning System  | 13 |
| Figure 2.6  | Circuit diagram for a system with different cooling loads  | 17 |
| Figure 2.7  | P-h diagram for a system with different cooling loads  | 17 |
| Figure 2.8  | Circuit diagram for system with similar cooling loads  | 18 |
| Figure 2.9  | P-h diagram for system with similar cooling loads  | 18 |
| Figure 3.1  | Layout of the YCC60C   | 24 |
| Figure 3.2  | Schematic circuit for evaporator-condenser system  | 25 |
| Figure 3.3  | P-h Diagram for the evaporator-condenser system  | 25 |
| Figure 3.4  | Psychometric chart for the evaporator-condenser system   | 27 |
| Figure 3.5  | CoilDesigner user interface  | 29 |
| Figure 3.6  | Vapcyc user interface  | 30 |
| Figure 3.7  | Inside of the YCC60C   | 33 |
| Figure 3.8  | Cone-shaped type distributors  | 35 |
| Figure 3.9  | Distributor and header piping of the cooling coil and reheat coil  | 36 |
| Figure 3.10 | Electronic expansion valve   | 38 |
| Figure 3.11 | Solenoid valve   | 38 |
| Figure 3.12 | Check valve  | 38 |
| Figure 3.13 | Piping and components of the evaporator-condenser system   | 39 |
| Figure 3.14 | Schematic of the nozzle airflow measuring apparatus  | 40 |
| Figure 3.15 | Loop air enthalpy test method arrangement  | 41 |
| Figure 3.16 | Charge optimization of YCC60C  | 43 |
| Figure 4.1  | Effect of entering reheat coil temperature on total capacity and absolute humidity   | 52 |
| Figure 4.2  | Evaporator saturation temperature against entering reheat coil temperature   | 52 |

|              |   |    |
|--------------|---|----|
| Figure 4.3   | Sensible and latent heat removal  | 53 |
| Figure 4.4   | Total capacity and power input against entering reheat coil temperature | 54 |
| Figure 4.5   | Coefficient of performance against entering reheat coil temperature     | 55 |
| Figure 4.6   | Effect of entering reheat coil temperature on relative humidity         | 56 |
| Figure 4.7   | Air leaving dry bulb temperature  | 57 |
| Figure 4.8   | Simulation and test comparisons   | 58 |
| Figure 4.9   | Refrigerant mass flow rate  | 60 |
| Figure 4.10  | Suction and discharge temperatures                                      | 62 |
| Figure 4.11A | P-h diagram for entering reheat coil temperature at 21.0°C              | 63 |
| Figure 4.11B | P-h diagram for entering reheat coil temperature Reheat at 33.8°C       | 64 |
| Figure 4.11C | P-h diagram for entering reheat coil temperature Reheat at 43.0°C       | 64 |
| Figure 4.12  | Variation of moisture removal capacity with air flow rate               | 65 |
| Figure 4.13  | RH reduction vs fan speed (THX)   | 66 |

## NOMENCLATURE

|                       |   |
|-----------------------|---|
| COP                   | Coefficient of performance [-]                        |
| $C_{p,air}$           | Air specific heat capacity [kJ/kg.K]                  |
| CSC                   | Constant speed compressor [-]                         |
| DB                    | Dry bulb temperature of air [°C]                      |
| EXV                   | Electronic expansion valve [-]                        |
| $h_{air,inlet}$       | Air enthalpy at inlet [kJ/kg]                         |
| $h_{air,outlet}$      | Air enthalpy at outlet [kJ/kg]                        |
| $\Delta h_{air}$      | Air enthalpy difference [kJ/kg]                       |
| $\Delta h_{comp}$     | Refrigerant enthalpy difference at compressor [kJ/kg] |
| $h_{comp,inlet}$      | Refrigerant enthalpy at compressor inlet [kJ/kg]      |
| $h_{comp,outlet}$     | Refrigerant enthalpy at compressor outlet [kJ/kg]     |
| $\Delta h_{ref,evap}$ | Refrigerant enthalpy difference at evaporator [kJ/kg] |
| $h_{evap,inlet}$      | Refrigerant enthalpy at evaporator inlet [kJ/kg]      |
| $h_{evap,outlet}$     | Refrigerant enthalpy at evaporator inlet [kJ/kg]      |
| $\dot{m}_{air}$       | Air mass flow rate [kg/s]                             |
| $\dot{m}_{ref}$       | Refrigerant mass flow rate [kg/s]                     |
| P                     | Pressure [MPa]  |
| $P_{comp}$            | Compressor power [W]                                  |
| $P_{fan}$             | Fan power [W]   |
| $P_{total}$           | Total power input [W]                                 |
| $Q_{cooling,air}$     | Cooling capacity based on air [W]                     |
| $Q_{cooling,ref}$     | Cooling capacity based on refrigerant [W]             |
| $Q_{latent}$          | Latent heat capacity [W]                              |
| $Q_{sensible}$        | Sensible heat capacity [W]                            |

|                         |                                  |
|-------------------------|----------------------------------|
| $\Delta T_{\text{air}}$ | Air temperature difference [K]   |
| TXV                     | Thermostatic expansion valve [-] |
| VAV                     | Variable air volume [-]          |
| VSC                     | Variable speed compressor [-]    |
| W                       | Humidity ratio [-]               |

**Greek Subscripts**

|        |  |
|--------|--|
| $\eta$ | Air-refrigerant heat transfer efficiency [-] |
|--------|--|



## CHAPTER I

### INTRODUCTION

The human body constantly generates heat all through the day. Vigorous activities will cause the body to generate more heat compared to a person at rest. Because there are many conditions where the human body will generate different amounts of heat, comfort conditions are difficult to generalize. The body will feel comfortable if it is able to dissipate the excess heat to the environment.

Human comfort conditions are subject to three primary factors i.e. temperature, relative humidity and air motion [1]. By isolating each factor, a better explanation is given for the effect of each factor on the thermal comfort.

Heat transfer can only happen when there is a temperature difference between two bodies. In thermal comfort, the human body has to be able to dissipate heat to the surrounding air in summer or to gain heat from heated surroundings in winter. If the temperature of the air is too low, the human body rapidly loses heat to the air, hence will feel cold. To prevent the human body from losing heat, it can be insulated by wearing thicker clothes. On the other hand, if the temperature of the air is too high, there is inadequate difference, or even an adverse difference, in temperature between the human body and the surroundings. As a result, the body is unable to reject heat effectively, which leads to a feeling of discomfort. To promote heat transfer from the human body to air in warm climates, the heat transfer has to be augmented either by perspiration or by introducing air motion.

Perspiration is one of the human body's natural responses to warm environments. When the heat from the human body is not dissipated quickly enough, the human body perspires. Due to the latent heat of evaporation of water, the body feels cool once the sweat evaporates. The rate of evaporation is dependent on the relative humidity of the surrounding air. If the surrounding air is saturated with water,

the relative humidity is high and the air is unable to take in any more water. The sweat cannot evaporate and the human body is unable to dissipate heat by perspiring. At the same air temperature, a person will feel cooler at lower air humidity compared to higher air humidity.

Introducing air motion around a person augments the heat transfer rate from the body to the surrounding air in warm environments. The heat transfer coefficient of air is directly proportional to air velocity. Using blowers or fans to promote air motion helps the human body to dissipate heat to the air, hence cooling the body. The use of blowers and fans increase the heat transfer from the human body to the air and therefore, it is not suitable for use in cooler environments.

ASHRAE Standard 55 describes a method to define a condition for thermal comfort that is acceptable to at least 80% of the occupants [2]. This method takes into account environmental factors as well as personal factors, such as activity and clothing. Generally, the temperature and relative humidity ranges for comfort are between 20°C to 26°C and 30% to 60% respectively.

Typical air conditioning systems require user input for controlling the air dry bulb temperature. Being able to control the temperature allows the user to select a temperature at which he/she can feel comfortable. The user is also able to select the desired fan speed. However, most air conditioning systems do not have a method of control for relative humidity. Although the air conditioning systems provide dehumidification, it is a by-product of cooling the air and cannot be directly controlled.

The concept of relative humidity control of air, by first cooling the air to reduce absolute humidity and then reheating it, is quite common and used widely in dehumidifiers. Cooling the air will result in moisture removal and lower absolute humidity whereas reheating the air will result in a lower relative humidity. In air conditioning systems, different methods are used to achieve the reheat effect e.g. auxiliary heater, desiccant wheel and heat pipes. The techniques stated utilize external methods to control the humidity of the air. It is proposed that the current refrigerant circuit in the air conditioning system be modified to integrate humidity control into the system, rather than use separate systems to first cool and then heat the air.

Therefore, a study is first performed for this modified air conditioning system to examine its feasibility.

### **1.1 Justification for the Research**

The main purpose of air conditioning is to supply air at a comfortable level to living spaces as defined by ASHRAE Standard 55 [2]. This is achieved by absorbing heat from the indoor air and rejecting the heat through a condenser in the cooling mode of operation. This will lower the indoor temperature to a comfortable level. However, as the air cools down, the relative humidity of the air rises. A relative humidity of more than 70% will cause fungal contamination. High humidity supports the growth of pathogenic or allergenic organisms [2]. High relative humidity also prevents cooling of the human body by evaporation of perspiration. If the human body is unable to dissipate heat, the person will experience thermal discomfort.

In addition to that, controlling the temperature of the air entering a space is also important for providing thermal comfort. This control method is already available in most air conditioning systems. However, relative humidity control along with temperature control is not available in conventional air conditioning units.

Equipment for humidity control can be very costly or not space efficient. Certain equipment, e.g. heater, is not energy efficient as well. With these drawbacks in mind, the purpose of this research is to study the feasibility of incorporating humidity control to an existing air conditioning unit. The method for introducing humidity control is by adding a reheat coil to the unit, which is connected in series before the evaporator coil. Humidity control can be achieved using an electronic expansion valve to regulate the refrigerant temperature at the reheat coil.

## 1.2 Objectives of Study

In this study, an evaporator-condenser system based on the two-evaporator air conditioning system is to be used in order to control the relative humidity of air leaving the system. The objective of the study is to investigate the effects of adding a condenser or reheat coil to the indoor unit in terms of coefficient of performance (COP), cooling capacity, absolute humidity and relative humidity of the leaving air.

## 1.3 Scope of Study

The evaporator-condenser system study is to be performed using the York brand ceiling concealed indoor unit YCC60C as shown in Figure 1.1. The outdoor condensing unit shall be the York brand YSL61C as shown in Figure 1.2, with a capacity of 6 hp. R410a is to be used as the refrigerant. The compressor and blower are constant speed types.

The existing YCC60C has a 3-row indoor coil as the evaporator. An additional row will be placed in the unit to serve as the reheat coil. The reheat coil is installed in series with the cooling coil. The degree of reheat is controlled by changing the refrigerant pressure by means of an electronic expansion valve.

The entering conditions for air side as per the ISO standards [3] for standard indoor cooling conditions are as follows:

|                               |    |
|-------------------------------|----|
| Air Dry Bulb Temperature (°C) | 27 |
| Air Wet Bulb Temperature (°C) | 19 |

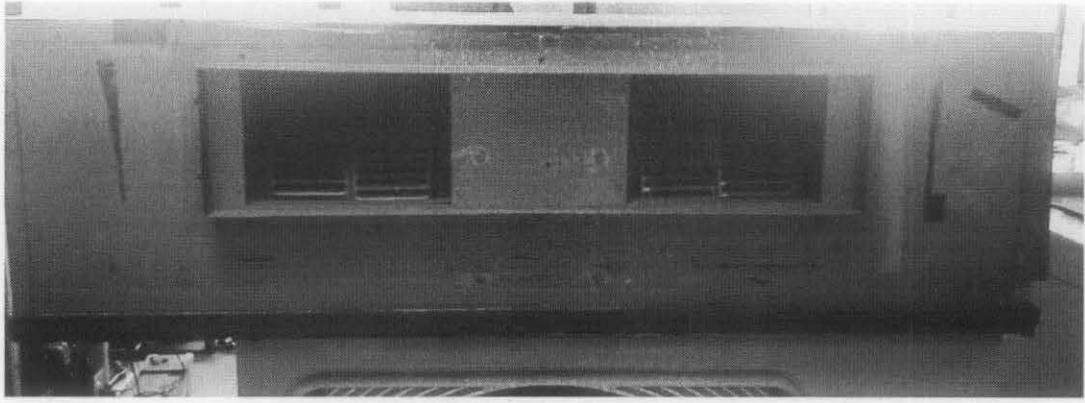


Figure 1.1: York ceiling concealed indoor unit YCC60C

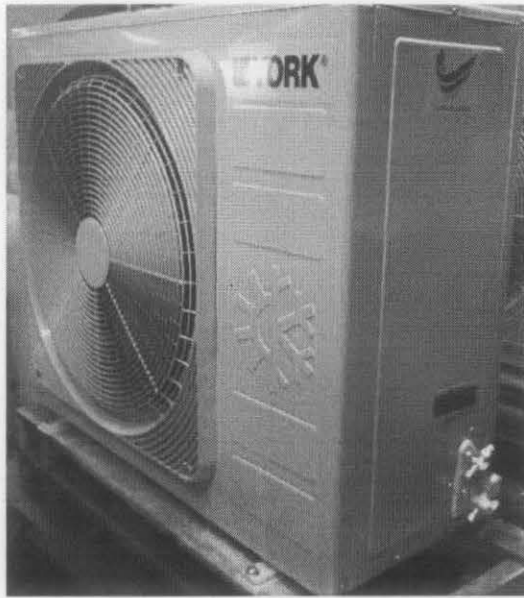


Figure 1.2: York outdoor condensing unit YSL61C

## CHAPTER II

### LITERATURE REVIEW

#### **2.0 Chapter Overview**

In this section, a background study on thermal comfort and some of the common methods to control humidity are discussed in order to compare the advantages and disadvantages of the proposed evaporator-condenser system. The current applications of the two-evaporator system are also discussed.

#### **2.1 Thermal Comfort**

The criteria for thermal comfort were briefly mentioned in Chapter 1. They include temperature, relative humidity and air motion. ASHRAE Standard 55 [2] provides a detailed explanation regarding thermal comfort but it is by no means an exhaustive source of information. This is because each individual has different perception of the thermal environment and therefore the range of thermal comfort is based on a 10% dissatisfaction criterion. The purpose of the standard is to “specify a thermal environment that is acceptable to at least 80% of the occupants”. The acceptable ranges of operative temperature and humidity based on the PMV-PPD index are shown in Figure 2.1.

In addition to achieving thermal comfort, simulation and experimental studies have reported that thermal comfort control can also produce higher energy efficiency and system reliability [4, 5, 6].

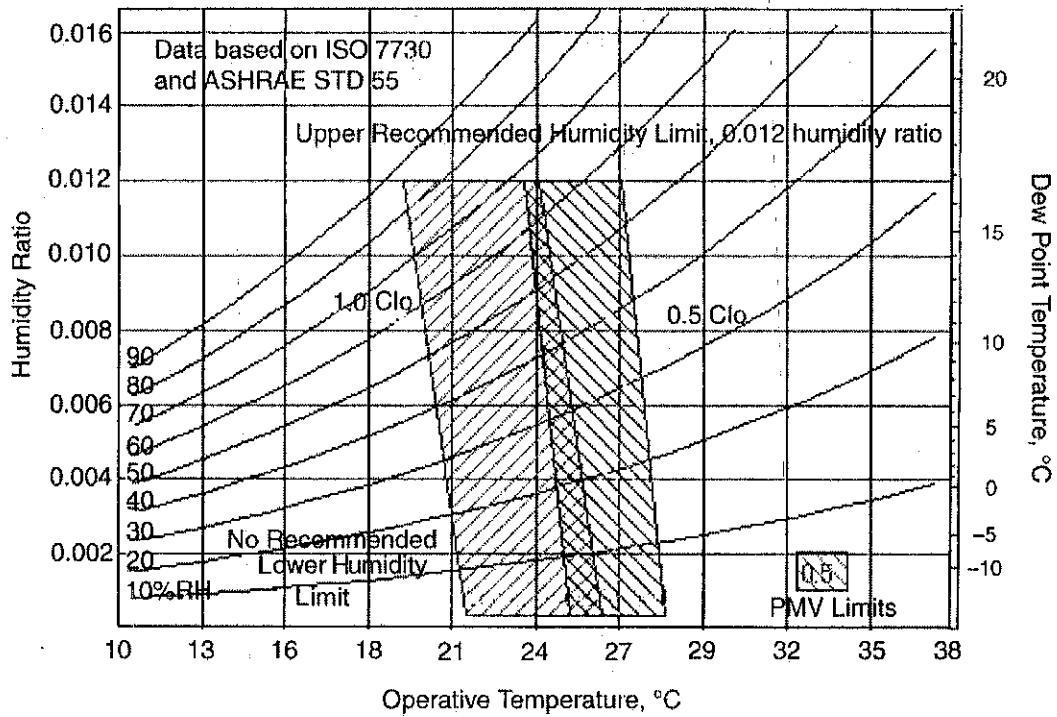


Figure 2.1: Acceptable ranges of operative temperature and humidity based on a 10% dissatisfaction criteria for general (whole body) thermal comfort based on the PMV-PPD index, plus an additional 10% dissatisfaction that may occur on average from local (partial body) thermal discomfort [2]

### *2.1.1 Thermal Comfort Index*

Rather than using environmental parameters such as air temperature or humidity for controlling the operation of A/C systems, using thermal comfort index is also possible. Two such indexes are Fanger's mathematical models predicted mean vote (PMV) and predicted percentage dissatisfied (PPD) [7, 8]. Fanger's PMV model combines four physical variables (air temperature, air velocity, mean radiant temperature, and relative humidity), and two personal variables (clothing insulation and activity level) into an index that can be used to predict the average thermal sensation of a large group of people in a space. The PMV describes the quality of thermal environment as a mean value of votes of a large group of people. The PPD describes the thermal comfort level as a percentage of thermally dissatisfied people. Fanger's PMV-PPD thermal comfort index is widely used and accepted for design and field assessment of thermal comfort [9, 10, 11, 12, 13]

## **2.2 Humidity Control**

Humidity control is an integral part of air conditioning and thermal comfort, the other being temperature control. To achieve moisture removal, the cooling coil surface temperature must be below the dew point of the air being cooled. The cooling coil surface temperature is dependant on the refrigerant evaporating temperature. From the refrigerant point of view, a lower refrigerant evaporating temperature will result in more moisture removal. Referring to the coefficient of performance (COP) of the Carnot Cycle, a higher evaporating temperature will result in a higher COP. Therefore the higher rate of moisture removal by means of lower evaporating temperature comes at the cost of lower COP.

### *2.2.1 Dehumidifier*

For situations where a lower air temperature is not required, a dehumidifier can be used to control humidity. A dehumidifier consists of an evaporator, condenser,



compressor and a fan in one unit as shown in Figure 2.2. In this configuration, the air is drawn through the unit via the fan into the evaporator. At the evaporator, the air is cooled to below the dew point and moisture is removed. After that, the cooler and drier air is passed through the condenser where it is reheated to the space temperature before being discharged into the space. The compressor work is also absorbed by the indoor air in this case, resulting in a higher air temperature compared to the inlet. Dehumidifier capacity is determined by the amount of moisture it can remove under given inlet conditions of the air [14].

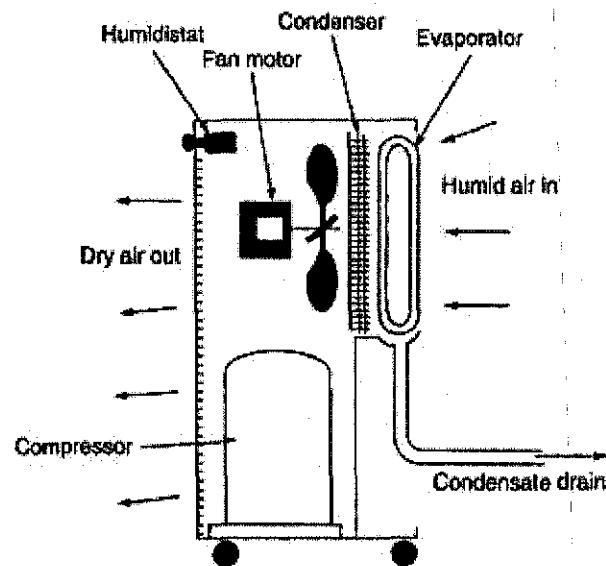


Figure 2.2: Schematic of a dehumidifier [14]

### 2.2.2 Auxiliary Heater

For central air conditioning systems found in buildings, humidity control can be achieved by overcooling the air, thereby removing more moisture, and then reheating the air using an auxiliary heater. Referring to Figure 2.3, the evaporator coil first cools the air until its temperature is lowered below its dew point, thereby removing moisture from the air and dehumidifying it. After that, the cooled air is reheated by an auxiliary heater to a more comfortable temperature to cater for the room cooling load. Without the auxiliary heater, it is possible that the room will be overcooled, creating an uncomfortable environment. Although this method is able to achieve the objective

of humidity control, it is not energy efficient on account of the additional heating energy input. As a result of the higher energy consumption, the COP of the system is lower [15]. The energy requirement for subcooling with reheat can be typically 1.65 times the requirement to just cool the air to its delivery temperature [16]. Furthermore, this system is difficult to implement in direct expansion (DX) air conditioning systems due to size constraints.

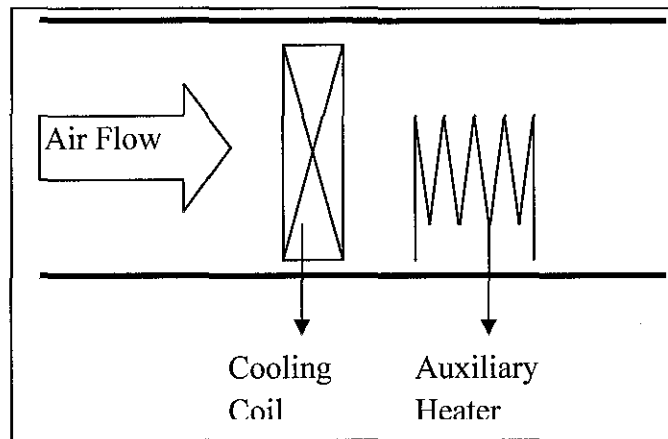


Figure 2.3: Relative humidity control by auxiliary heater

An advantage that is present in central air conditioning systems is the availability of space. This allows various configurations of the air conditioning system to cater for humidity control. Specific dehumidification equipment, such as heat pipes or desiccant wheels, can be separately installed into the air ducts to provide additional moisture removal.

### 2.2.3 Desiccant Wheel

One of the more established methods for dehumidifying is using a desiccant wheel. The function of the desiccant wheel is to absorb water vapor from an air stream and transfer it out of the space. This is because desiccant chemical material is hydrophilic. Once the desiccant material is saturated with water, the water content is removed from the wheel using a stream of hot air, heated by direct fuel-firing, steam, hot water or waste heat [17].

Desiccant materials are divided into two categories i.e. regenerative and non-regenerative. Non-regenerative equipment uses hygroscopic salts such as calcium chloride, urea, or sodium chloride. Regenerative systems usually use a form of silica or alumina gel, activated alumina, molecular sieves, lithium chloride salt or solution, or glycol solution [18].

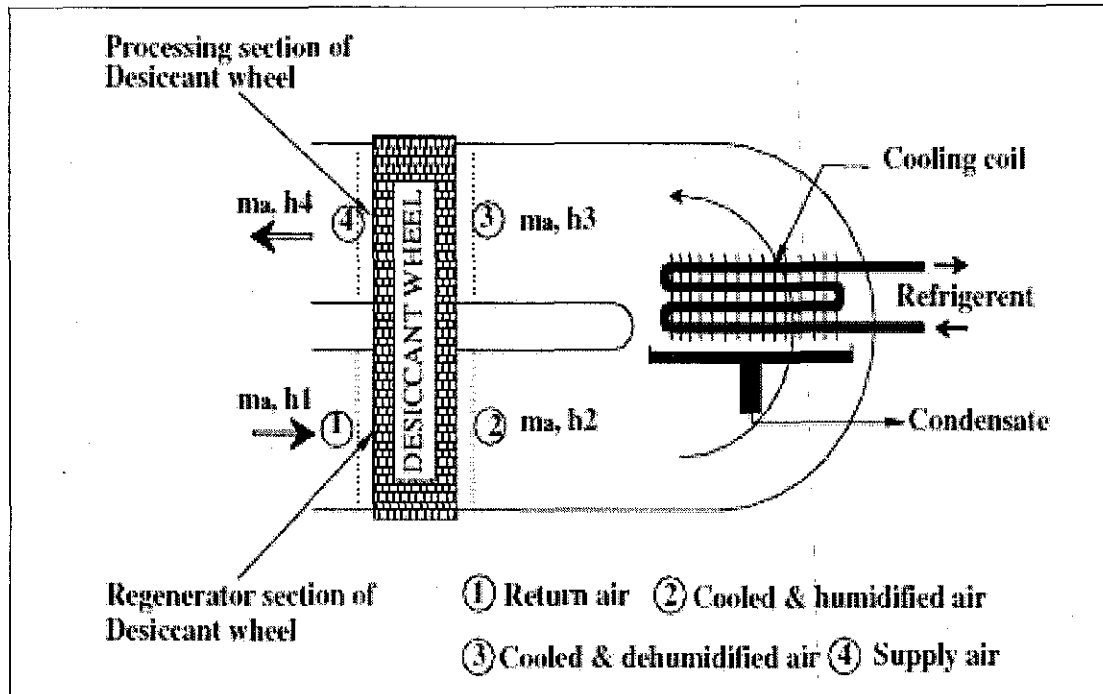


Figure 2.4: Schematic diagram of a desiccant wheel in an air-conditioning system [19]

Figure 2.4 shows the configuration for an air-conditioning system with a desiccant wheel. The desiccant material used is metal silicate synthesized on inorganic fiber substrate (net organics less than 2%). In general, the desiccant wheel is wrapped around the evaporator coil. The air to be cooled and dehumidified first enters the desiccant wheel where the wheel pre-cools and humidifies the air. Then the pre-cooled air enters the cooling coil where it will be further cooled and dehumidified. Before the cooled air enters the space to be conditioned, the desiccant wheel reheats and dehumidifies the air. Experimental studies show that the desiccant wheel is able to enhance the dehumidification of the air but has a lower COP compared to the conventional cooling system by 5% [19].

#### 2.2.4 Heat Pipe/Thermosyphon

Another way to provide dehumidification is by the heat pipe or thermosyphon. The heat pipe consists of two heat exchangers, namely the heat pipe evaporator and heat pipe condenser. The heat pipe is wrapped around the evaporator coil, where supply air is pre-cooled by the heat pipe evaporator and reheated by the heat pipe condenser. By pre-cooling the air before entering the evaporator coil, the sensible cooling load on the cooling coil is lower and therefore it is possible to remove more moisture. The heat pipe condenser reheats the cooled air to decrease the relative humidity. The heat is considered “free” because no external energy is required to reheat the cooled air [20].

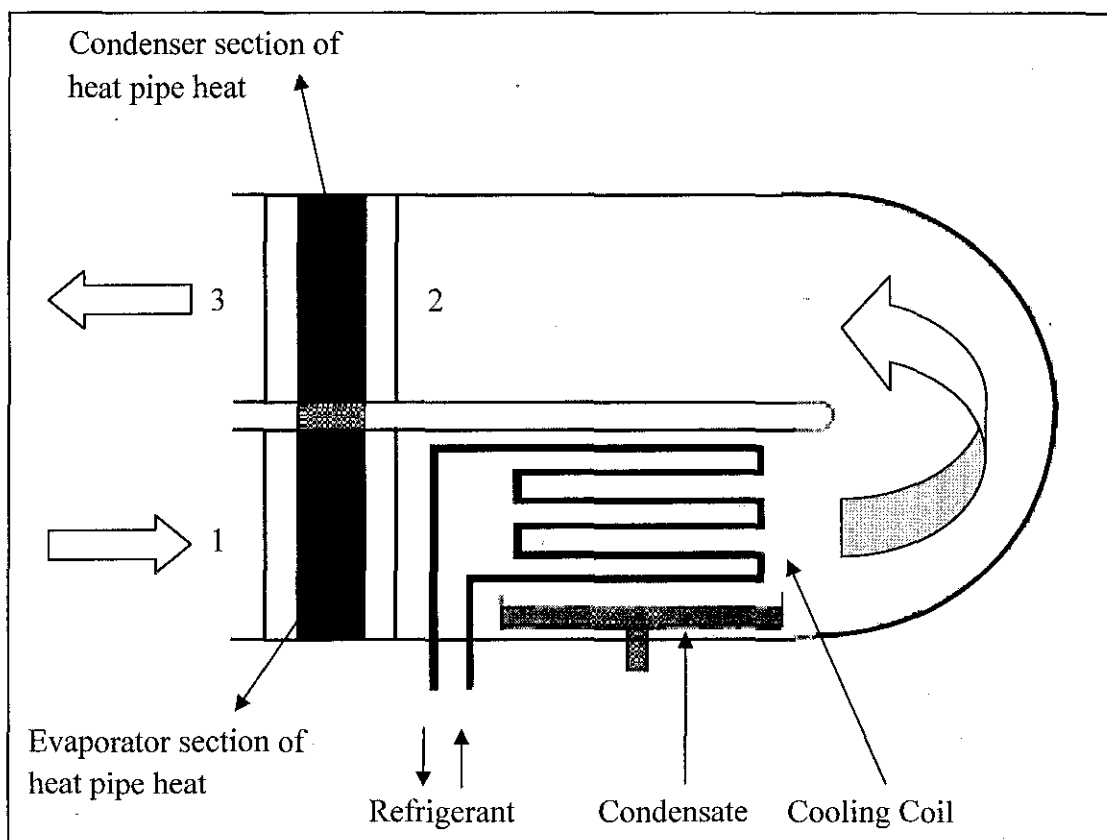


Figure 2.5: Schematic diagram of a heat pipe heat exchanger in an air conditioning system

The configuration for the Heat Pipe Heat Exchanger system as shown in Figure 2.5 is similar to that of the desiccant wheel system, where the desiccant wheel is replaced with the heat pipe heat exchanger. An experimental study [21] has shown that the cooling capability of the system is enhanced by 20% to 32.7% and the

condenser of the heat pipe heat exchanger is able to act as a heater to replace the conventional heater. However, the addition of the heat pipe heat exchanger increases air-side pressure losses, manufacturing cost and the overall size of the air conditioning unit. Furthermore, the claimed enhancement of the cooling capability of this system might have been misinterpreted. The cooling capacity is calculated from point 1 to point 2 and disregards the reheating of the air. For a more meaningful comparison, it is better to calculate the cooling capacity from point 1 to point 3, in which case the cooling capacity may become less than a straight system.

### *2.2.5 Constant Speed Compressors*

Attempts to control humidity using constant speed compressor (CSC) lead to several complications. The constant speed compressor relies on on-off functions to regulate the air temperature. During the off cycle, it has been demonstrated that moisture is added to the air stream [22]. During cooling mode, the compressor is switched on and moisture is removed from the air via condensation on the cold fins. The condensate water flows towards a drain pan where it is drained out. When the compressor is switched off, the coil is still cool and provides sensible cooling. In addition to the sensible cooling, accumulated moisture on the fins provides evaporative cooling, adding further moisture to the air. In such situations, there is no net enthalpy change across the coil [23]. While on-off compressors are not suitable to control the humidity, a H-L compressor with high and low speed settings was used along with a variable speed blower. The rationale for the change from CSC is to prevent the compressor from entirely turning off when the temperature is too low. The H-L compressor does not accurately control the humidity levels but is more cost effective compared to the variable speed compressor (VSC) [24], which is reviewed below.

Another method to avoid the occurrence of on-off cycles in CSC is to implement air bypass (BA) systems. Such system uses dampers for a portion of the air to bypass the cooling coil. The portion of air which enters the cooling coils is dehumidified and cooled. The cooled air is then mixed with the bypass air at a later point before entering the conditioned space. This method works well at maintaining

the room temperature, but due to the smaller amount of air entering the cooling coil, the humidity control is of a lesser extent compared to other systems [25].

### *2.2.6 Variable Speed Compressors and Blowers*

Controlling humidity via evaporating temperature requires a VSC i.e. inverter compressor. CSCs are unable to vary the evaporating temperature at a given condition. Typical CSCs control the temperature by switching on when the sensed temperature is too high, and switching off when the sensed temperature is too low. On the other hand, VSCs can provide better control by modulating the refrigerant mass flow rate. When more moisture removal is required, the refrigerant mass flow rate will be lowered in order to reduce the refrigerant evaporating temperature.

Humidity control can also be achieved by varying the air flow rate, such systems being termed variable air volume (VAV) systems. A lower air flow rate reduces the fin temperature and allows more moisture to be removed. In the VAV system, the cooling performance is poorer when more moisture is to be removed. This is due to the lower air volume being cooled. The lower air flow being treated will also cause the air to become stale due to smaller number of air changes and will also have a lower air motion, which is also a factor in thermal comfort [26].

A patent describes the use of two cooling coils to control humidity in building systems [27]. The first cooling coil is used to treat fresh air, which has a higher humidity. The cooled and dehumidified fresh air is then mixed with the return air, which is warmer. The resultant mixed air is then passed through the second cooling coil, where the air temperature is brought down to a more comfortable level before entering the room.

Experimental results have shown that humidity control using VSCs and supply fans can be accurately achieved [28, 29]. The ability to control the humidity comes from the various sensible heat factor (SHF) possibilities when varying the compressor and blower speeds [30]. A consequence of the lower refrigerant mass flow rate is the

poorer performance of the cooling system. Thus, humidity control comes at the sacrifice of cooling performance.

### **2.3 Current Two-Evaporator Applications**

A review of the current literature shows that a two-evaporator concept has been applied mainly in household refrigerators, where there are separate compartments requiring different cooling loads i.e. freezer and refrigerator section in one unit [31]. Referring to Figures 2.6 and 2.7, the refrigerant leaving the condenser goes through the first expansion valve (1-2) and into the first evaporator. The refrigerant absorbs heat from the space (2-3) and then enters the second expansion valve (3-4) and into the second evaporator (4-5) before returning to the compressor (5-6) and finally completing the cycle in the condenser (6-1). It can be said that the two evaporators are arranged in series. In this configuration, the cooling load for the first evaporator is less than the second evaporator.

In a more common configuration, the two-evaporator system is used for different spaces with the same cooling load [32]. Referring to Figures 2.8 and 2.9, the refrigerant leaving the condenser enters the first and second evaporator before expanding to the working pressure. It can be said that the two evaporators are arranged in parallel. The refrigerant absorbs heat from the spaces and returns to the compressor, finally releasing at the condenser all the heat absorbed in the evaporators, and completing the cycle.

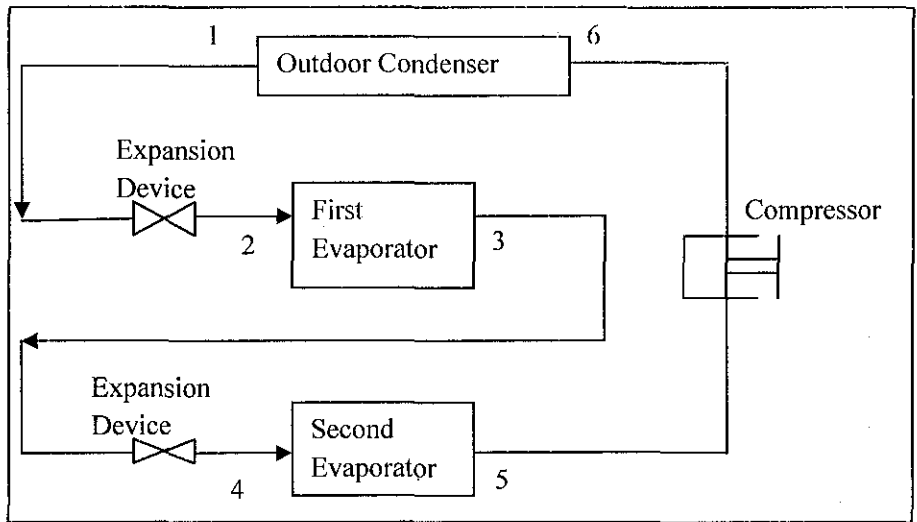


Figure 2.6: Circuit diagram for a system with different cooling loads

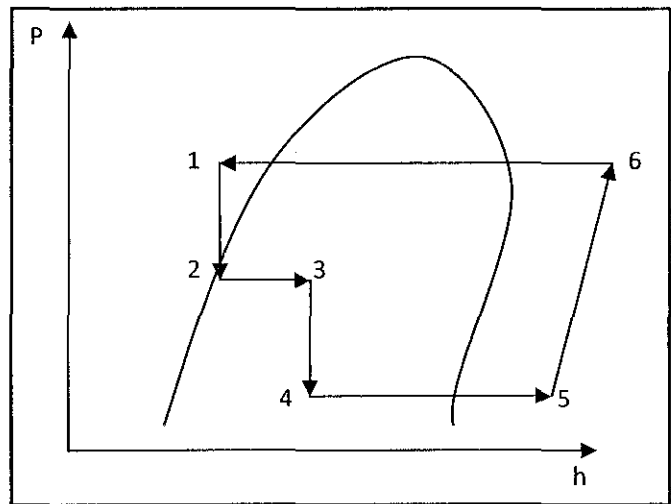


Figure 2.7: P-h diagram for a system with different cooling loads



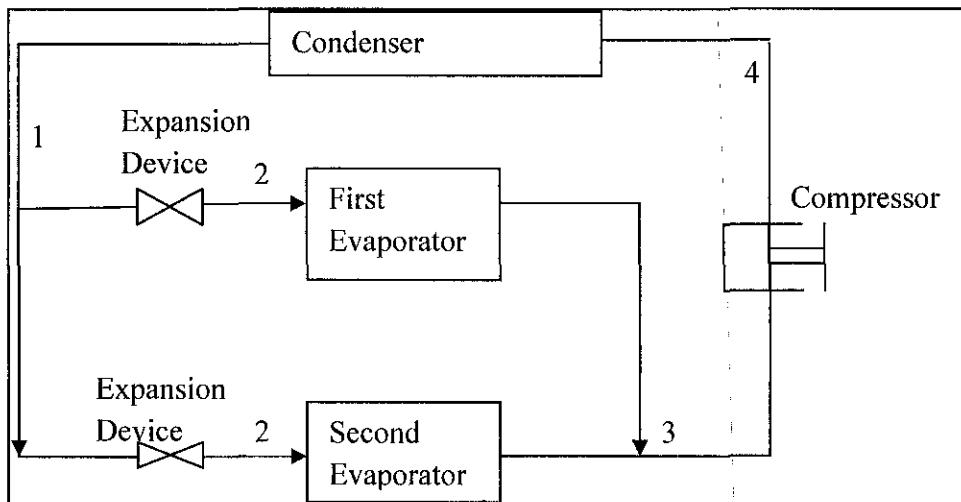


Figure 2.8: Circuit diagram for system with similar cooling loads

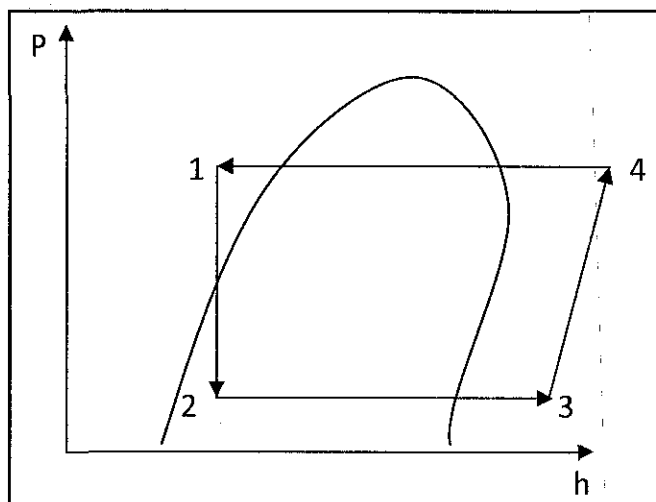


Figure 2.9: P-h Diagram for System with Similar Cooling Loads

A study conducted using two evaporator refrigerator using non-azeotropic refrigerant R22/R11 in series and one capillary tube as expansion device (Known as the Lorenz-Meutzner cycle) shows a power saving of up to 20% compared to a conventional refrigerator using R12 [33]. The Lorenz-Meutzner cycle uses a refrigerant blend with a large temperature glide. A similar study also yielded the same results [34]. A computer simulation of two-evaporator refrigerating system charged with pure and mixed refrigerants shows a significant increase in COP [35]. An experimental study on a modified Lorenz-Meutzner cycle with bypasses to the

compressor shows that the energy saving potential is high when two-evaporators are used in series [36, 37].

## **2.4 Opportunities for Research**

A review on the state of the art in humidity control shows that humidity control can be achieved using various methods. External methods include the additional of humidity control equipment such as auxiliary heaters, desiccant wheels and heat pipes. The employment of dedicated cooling coils can also be used in central air conditioning system ducts to cater for humidity control, where the higher humidity from fresh air is removed and then mixed with return air. The mixed air is then further cooled to a more comfortable temperature. These external methods are suitable for large systems, where there is ample space to install the desired method.

Methods relating to the control of the air conditioning internal system can also be used for humidity control. Such methods include VAV and VSC systems which are able to accurately control the humidity at design conditions. The VAV and VSC systems require fine tuned algorithm and means to vary the speeds of the blower and compressor respectively. Unfortunately, the equipment for speed control is not cost effective. Although the VAV and VSC system for humidity control can be integrated as a unitary system, it may come at a premium price due to the more expensive equipment required.

In situations where cooling is not required, dehumidifiers can be used to remove moisture. As dehumidifiers can only remove moisture, it can only cater to one of the thermal comfort conditions.

Current two evaporator systems are used in applications where similar or different cooling loads are required. When similar cooling loads are required, the user is able to control each evaporator individually when needed. Systems with different cooling loads can use the two evaporator system with the advantage of a single compressor to save cost and space. The Lorenz-Meutzner cycle has shown to improve power savings up to 20%.

A solution is required to provide humidity control in areas where available space and costs are challenged. By modifying the two-evaporator system, a reheat effect can be provided to the air leaving the air conditioner. The aim of this study is to control humidity of the leaving air of a CSC commercial ceiling concealed unit using a reheat coil which is connected in series with the existing cooling coil. The working pressure of the reheat coil will be controlled using an electronic expansion valve. The expected system will be compact enough to use as a unitary system at a minimal increase in cost due to the relative simplicity of the system.

A brief summary of the methods for dehumidification and two-evaporator systems are shown in Table 2.1.

Table 2.1: Summary of common dehumidification methods

| Method                     | Advantages  | Disadvantages   |
|----------------------------|---|---|
| Dehumidifier               | <ul style="list-style-type: none"> <li>• Portable</li> <li>• Smaller unit</li> </ul>  | <ul style="list-style-type: none"> <li>• Discharged air is not cooled</li> </ul>  |
| Auxiliary Heater           | <ul style="list-style-type: none"> <li>• Reheat can be controlled</li> </ul>  | <ul style="list-style-type: none"> <li>• External energy required</li> <li>• Poorer COP due to additional energy to operate the heater</li> </ul>   |
| Desiccant Wheel            | <ul style="list-style-type: none"> <li>• Enhances the dehumidification of the air</li> </ul>  | <ul style="list-style-type: none"> <li>• lower COP compared to the conventional cooling system by 5%</li> </ul>   |
| Heat Pipe/<br>Thermosyphon | <ul style="list-style-type: none"> <li>• Cooling capability enhanced by 20% to 32.7%</li> </ul>   | <ul style="list-style-type: none"> <li>• Increased air side pressure losses</li> <li>• Increased manufacturing cost</li> <li>• Increased overall size of the air conditioning unit</li> </ul> |
| VSC and VAV system         | <ul style="list-style-type: none"> <li>• Able to control humidity accurately at design conditions</li> <li>• Unitary system</li> </ul>                                    | <ul style="list-style-type: none"> <li>• Not cost effective due to expensive equipment</li> <li>• Complex algorithm required</li> </ul>   |
| Two-Evaporator             | <ul style="list-style-type: none"> <li>• Used in refrigerators with freezer compartment</li> <li>• Different operating temperatures for different compartments</li> </ul> | <ul style="list-style-type: none"> <li>• Additional components such as expansion devices and heat exchangers needed</li> <li>• Power savings up to 20% in Lorenz-Meutzner cycle</li> </ul>    |

## **2.5 Chapter Summary**

A literature review has been done to determine the available methods for humidity control. The review has shown that the equipment for humidity control either requires large space, high costs or dedicated equipment. The two-evaporator system is examined for its potential use to control humidity. This research examines the use of the modified two-evaporator system as a compact system with minimal cost increase.

## CHAPTER III

### METHODOLOGY

#### **3.0 Chapter Overview**

This chapter describes the methods used for the study. This includes the basis for choosing the test units, preliminary calculations using CoilDesigner [38] and Vapcyc [39], necessary modifications made to the test unit and finally the testing procedures. The test procedures are divided into two sections: charge optimization and humidity control test. The result of the refrigerant charge optimization is also presented in this chapter.

#### **3.1 System Circuit Design**

The YCC60C indoor unit is chosen for this study because of its coil design. The endplate design for the heat exchanger allows sufficient space to add another row without any major modification to its current structure. A simple representation of the YCC60C layout is shown in Figure 3.1.

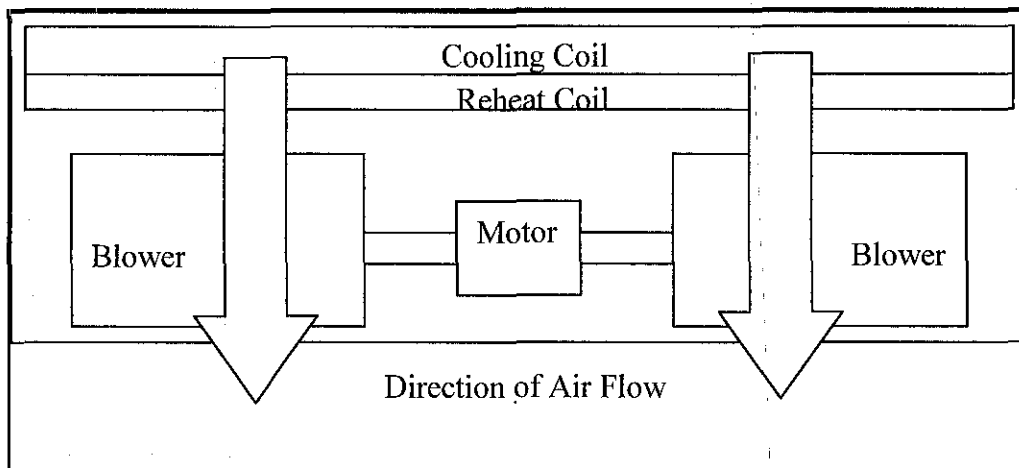


Figure 3.1: Layout of the YCC60C

The YCC60C has a large aspect ratio. In order to provide uniform distribution of air flow, two blowers are employed to draw air through the coils.

In this modified system, the first coil is a cooling coil which functions as an evaporator in a conventional air-conditioning system. The second coil carries the refrigerant mixture produced by EXV1 and is at a higher temperature compared to the evaporator coil. Thus it serves to reheat the cooled air leaving the first evaporator. This will eliminate the need for the heater and will provide the user a method to control the relative humidity leaving the air-conditioner. Due to the reheat function of the second coil, it shall be called the Reheat Coil to differentiate it from the outdoor condenser. The circuit diagram of the proposed evaporator-condenser system is shown in Figure 3.2.

Referring to the Figure 3.3, the refrigerant leaving the condenser will be in a sub-cooled liquid state (Point 1). The refrigerant at EXV1 will expand to the reheat coil working pressure of  $P_2$ . Air leaving the evaporator will absorb the heat from the refrigerant at the reheat coil and the enthalpy state of the refrigerant will move towards point 3. Refrigerant at Point 3 will then expand again at EXV2 to the working pressure of the evaporator at Point 5. From Point 4 to Point 5, the refrigerant absorbs heat from the air, thereby cooling the air. Point 5 corresponds to the refrigerant entering the compressor and finally, releasing the heat at the outdoor condenser at

Point 6, completing the cycle. The potential increase in performance comes from the lower quality of the refrigerant that absorbs more heat in the evaporator because of a higher latent heat requirement. This allows the refrigerant to absorb more heat from the air. The heating of the air from the reheat coil is intended to bring the relative humidity of the cooled air within the comfort range.

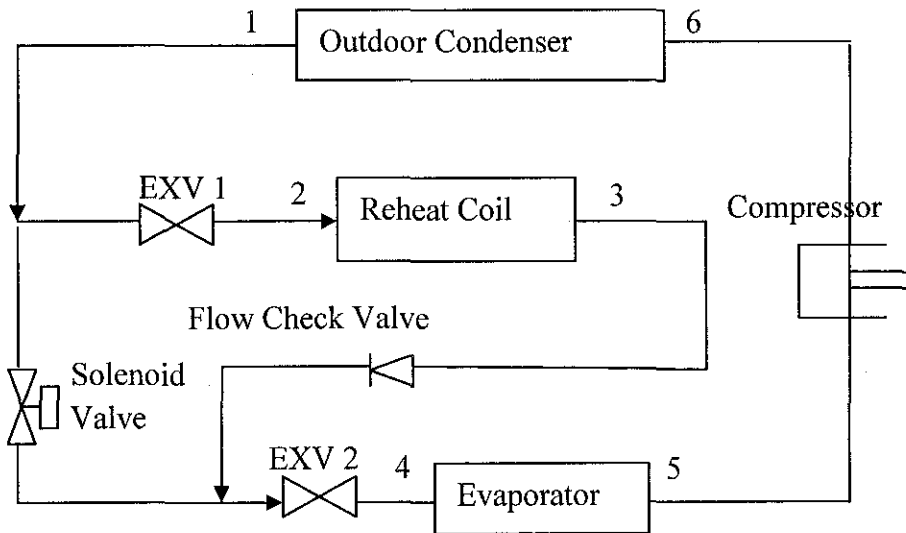


Figure 3.2: Schematic circuit for evaporator-condenser system

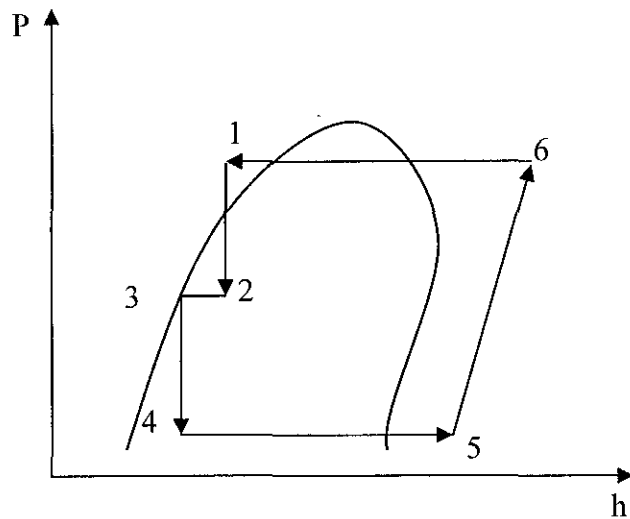


Figure 3.3: P-h Diagram for the evaporator-condenser system



The expected air conditioning process for the evaporator-condenser system plotted on a psychometric chart is shown in Figure 3.4: The conditions of air are based on the following to facilitate a better understanding of the process:

| Point | Dry Bulb Temperature (°C) | Wet Bulb Temperature (°C) | Humidity Ratio (g/kg) | Relative Humidity (%) |
|-------|---------------------------|---------------------------|-----------------------|-----------------------|
| 1     | 27                        | 19                        | 10.5                  | 47                    |
| 2     | 12                        | 11                        | 8.0                   | 90                    |
| 3     | 17                        | 13                        | 8.0                   | 65                    |

The air enters the evaporator at 27°C dry bulb temperature and 19°C wet bulb temperature. At the evaporator, the air is cooled and moisture is removed. The state of air leaving the evaporator is assumed to be at 12°C dry bulb temperature and 11°C wet bulb temperature. The cooled air is then heated at the auxiliary condenser to 17°C dry bulb temperature and 13°C wet bulb temperature. The absolute humidity of the heated air remains the same as the cooled air because of the sensible heating, but the relative humidity is lowered due to the increase in dry bulb temperature.

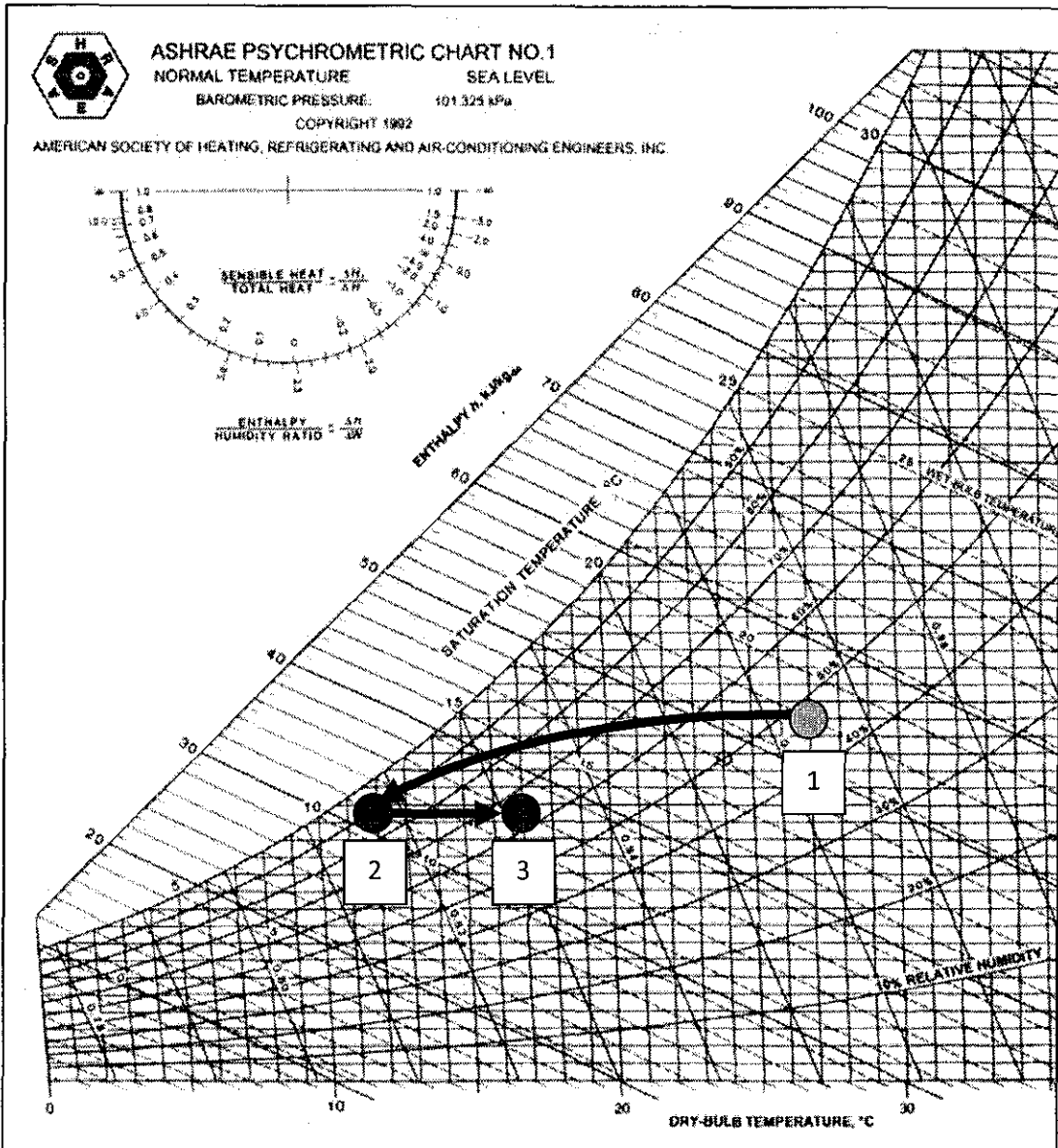


Figure 3.4: Psychrometric chart for the evaporator-condenser system

## 3.2 Vapcyc and CoilDesigner simulation

Before setting up the experimental apparatus, simulations are carried out to predict the performance of the unit. The simulation software used to perform these calculations are CoilDesigner and Vapcyc, both of which have been developed at the Center for Environmental Energy Engineering (CEEE), University of Maryland.

### 3.2.1 Method

CoilDesigner is a “general-purpose simulation and design tool” for predicting the performance of heat exchangers. Among the common types of heat exchangers available are fin-tube, microchannel and tube-in-tube. CoilDesigner is very flexible software and allows the user to choose from multiple correlations for heat transfer and pressure drop to best suit the purpose. There is also a variety of working fluids for the user to choose from. CoilDesigner is able to simulate the performance of a plate-fin-tube coil within  $\pm 10\%$  [38]. A screenshot of the CoilDesigner user interface is shown in Figure 3.5.

VapCyc is a tool for a steady-state vapor compression refrigeration system simulation and optimization [39]. The simulation focuses on a system consisting of a compressor, condenser, expansion device and evaporator connected in series. Evaporator and condenser coils designed in CoilDesigner are used as inputs in the Vapcyc along with the Compressor Performance Estimation Program (CPEP) to obtain a balanced system between the condenser, evaporator and compressor. A screenshot of VapCyc is shown in Figure 3.6.

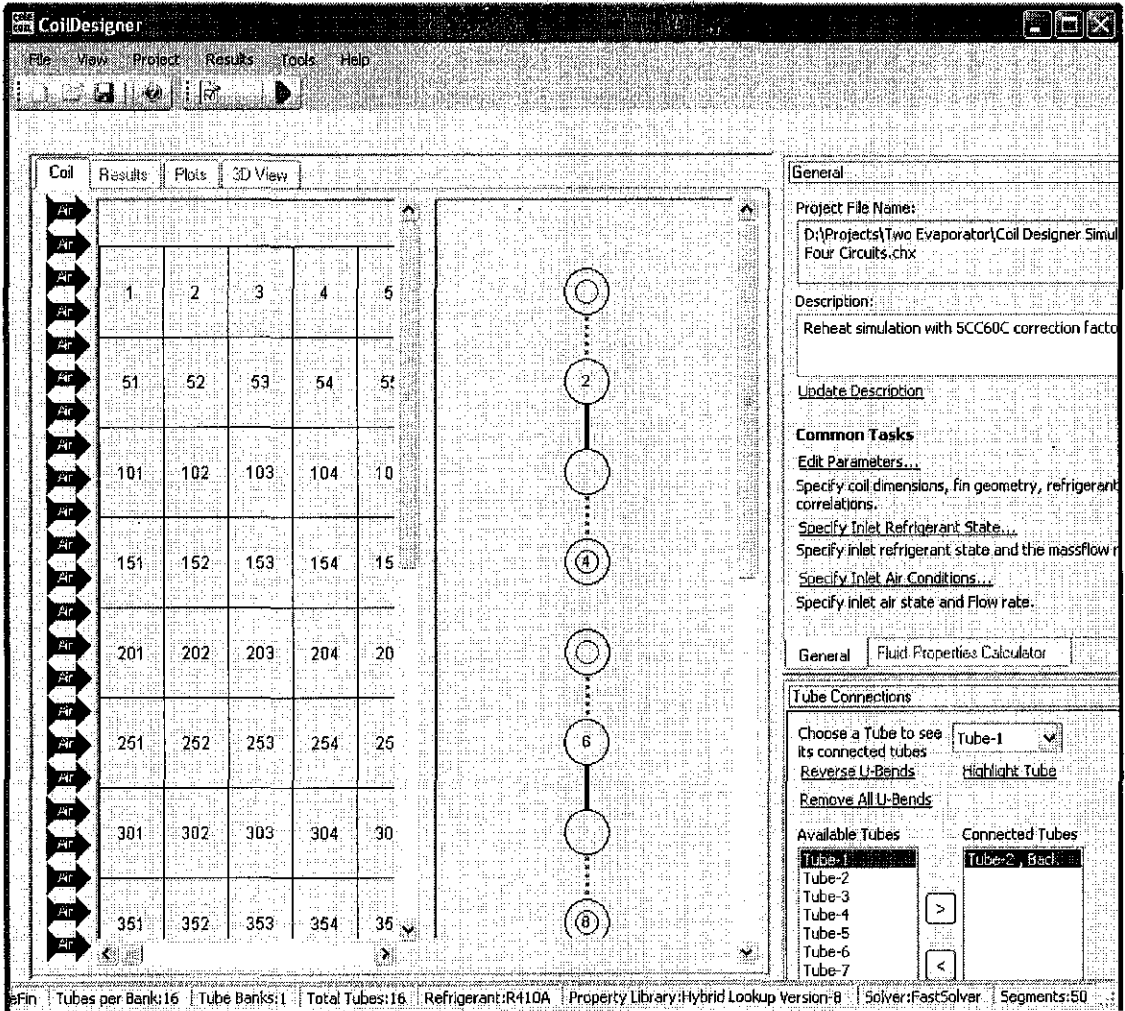


Figure 3.5: CoilDesigner user interface

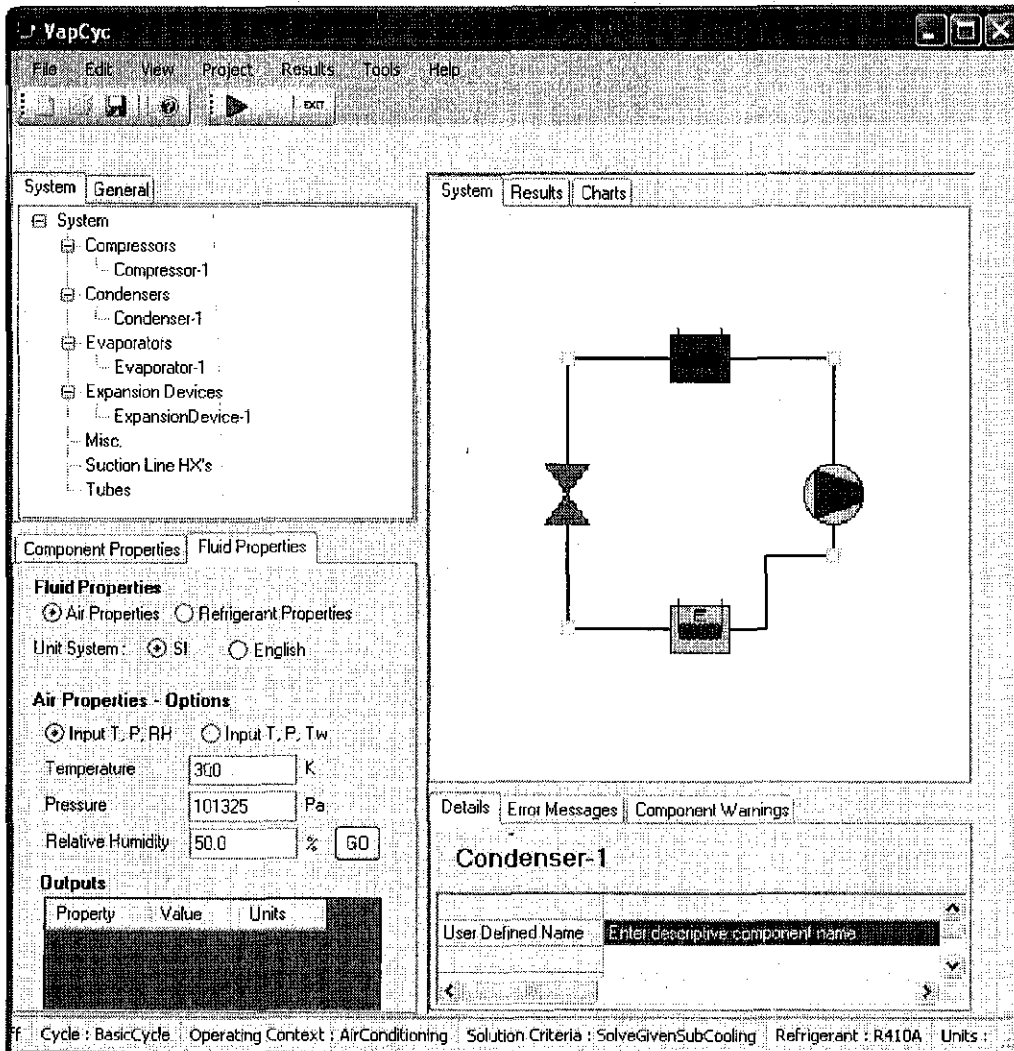


Figure 3.6: Vapcyc user interface

There are many aspects to consider when designing an air conditioning circuit. Among the critical ones are:

1. Condenser Size
2. Evaporator Size
3. Compressor
4. Refrigerant Charge
5. Expansion Device
6. Motor and Fan size

A change in any one of those items will result in involuntary change in others. With all these parameters, it is almost impossible to do a simulation. Therefore, some parameters need to be fixed as necessary inputs for simulation.

First, a balancing simulation (without the reheat coil) was performed using VapCyc. This balancing simulation is performed to obtain the cooling performance of the system without reheat. The results will serve as the simulation benchmark. The inputs required are the evaporator and condenser coil geometry, air flow rates for both evaporator and condenser, superheat temperature, subcool temperature and the compressor curve. The software first assumes a refrigerant mass flow rate and calculates the coil performance. The software then iterates the refrigerant mass flow rate until the superheat and subcool temperatures inputted earlier are achieved. For this simulation, the subcool is set at 5°C and the superheat at 7°C. The results of this balancing process are shown in Appendix A.

As the Vapcyc has a built in algorithm for straight cycles, its applicability to two-evaporator systems is unknown. CoilDesigner is used to simulate the reheat coil. To achieve the same air leaving dry bulb temperature as the benchmark, the air has to be over-cooled at the evaporator and then reheated at the reheat coil. This is achieved by lowering the evaporating temperature, thereby decreasing the air temperature leaving the evaporator, and then simulating the reheat coil effect on the air. In this

case, the inputs to the simulation are refrigerant pressure, refrigerant quality and refrigerant flow rate.

The cooling performance of the system can be estimated by calculating the enthalpy difference between the inlet and outlet air. The air enthalpy is a function of the air dry bulb, DB, and the humidity ratio, W. The enthalpy function is given as follows [40]:

$$h_{\text{air}} = 1.006 \times \text{DB} + W(2501 + 1.86 \times \text{DB}) \quad (3 - 1)$$

The air dry bulb temperature and wet bulb temperature can be obtained from the simulation results.

Knowing the enthalpy of the inlet and outlet air, the cooling performance can now be calculated by:

$$Q_{\text{total, air}} = \dot{m}_{\text{air}} \times (h_{\text{air, inlet}} - h_{\text{air, outlet}}) \quad (3 - 2)$$

The theoretical compressor power was obtained from the enthalpy difference between the outlet and inlet of the compressor. Referring to Figure 3.3, the points representing the inlet and outlet of the compressor are state points 5 and 6 respectively. Compressor power is calculated using the following equations:

$$P_{\text{comp}} = \dot{m}_{\text{ref}} \times \Delta h_{\text{comp}} \quad (3 - 3)$$

where

$$\Delta h_{\text{comp}} = h_{\text{comp, outlet}} - h_{\text{comp, inlet}} \quad (3 - 4)$$

Lastly, the coefficient of performance is calculated by:

$$\text{COP} = \frac{Q_{\text{total, air}}}{P_{\text{comp}}} \quad (3 - 5)$$

### 3.3 Experimental Setup

This section describes the specifications of the modified indoor unit YCC60C, components related to the indoor unit

#### 3.3.1 Indoor Unit

The indoor unit consists mainly of a cooling coil, reheat coil, two centrifugal blowers and a motor to drive the blowers. Figure 3.7 shows the inside view of the YCC60C.

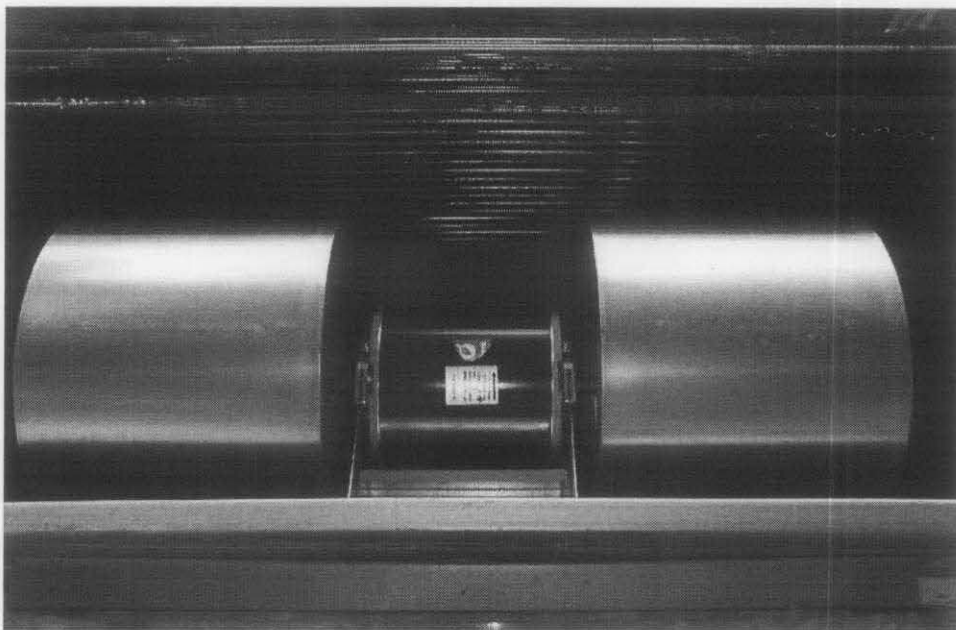


Figure 3.7: Inside view of the YCC60C



### 3.3.2 Cooling Coil and Reheat Coil

The cooling coil and reheat coil specifications are shown in Table 3.1.

Table 3.1: Cooling coil and reheat coil specifications

|                 | Cooling Coil     | Reheat Coil      |
|-----------------|------------------|------------------|
| Number of Rows  | 3                | 1                |
| Fins Per Inch   | 20               | 20               |
| Tube Height     | 16               | 16               |
| Fin Length (mm) | 1354.0           | 1354.0           |
| Fin Type        | Hydrophilic Slit | Hydrophilic Slit |

### 3.3.3 Motor and Blower

The power of the motor used to drive the blowers is 600 W. There are two blowers, each with a diameter of 214 mm and length of 203.2 mm.

### 3.3.4 Distributor

An important component used in fin-tube coils is the distributor. The function of the distributor is to evenly distribute the refrigerant flow into the individual circuits of the fin tube heat exchanger. A mal-distributed flow will result in poor heat exchanger performance. This is especially critical for two-phase flows where the liquid tends to stratify and flow towards the bottom circuits due to the gravitational effect, while the vapor remains at the top of the heat exchanger. There are several types of distributors used in the inlet of evaporator coils, i.e. Venturi, Cone-Shaped, and Round-Type. The type of distributor used for this study is the Cone- Shaped one. A picture of these

distributors is shown in Figure 3.8. It is used at the inlet of both the reheat coil and the evaporator coil.



Figure 3.8: Cone-shaped type distributors

A header pipe is used at the outlet of the reheat coil and evaporator coil.

The distributor and header piping of the indoor coils are shown in Figure 3.9.



Figure 3.9: Distributor and header piping of the cooling coil and reheat coil

### 3.3.5 *Electronic Expansion Valve*

The function of the expansion device in an air conditioning system is to control the working pressure of the evaporator. Common expansion devices include capillary tubes, thermostatic expansion valves (TXV) and electronic expansion valves (EXV). The evaporator-condenser system requires different pressures for the evaporator and the reheat coil. The expansion device used will be EXV. It is chosen because the degree of expansion can be set at a precise opening to control the working pressure of the coils. The EXV used is shown in Figure 3.10.

### 3.3.6 Solenoid Valve

Solenoid valves are used as an on-off switch to control the flow. The on-off switch is a magnetized coil which will open or close (Depending on Valve Type) via a plunger when the coil is energized. These valves are usually Normally Open (NO) or Normally Closed (NC). In a NO solenoid valve, the valve is opened and allows flow when the magnetized coil is de-energized and closed when the magnetized coil is energized, thereby blocking flow. In a NC solenoid valve, the valve is closed and thereby blocking flow when the magnetized coil is de-energized, and opened and allows flow when the magnetized coil is energized. The solenoid valve used is a NC type and is shown in Figure 3.11.

### 3.3.7 Check Valve

A check valve is used to control the direction of flow. In this study, the check valve allows refrigerant to flow from the reheat coil to the evaporator, but not in the opposite direction. The check valve used in this study has a nominal size of 12.7 mm (1/2"). It is shown in Figure 3.12.

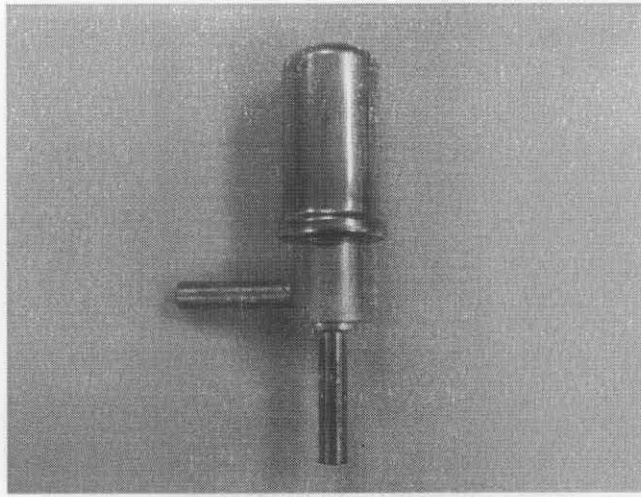


Figure 3.10: Electronic expansion valve

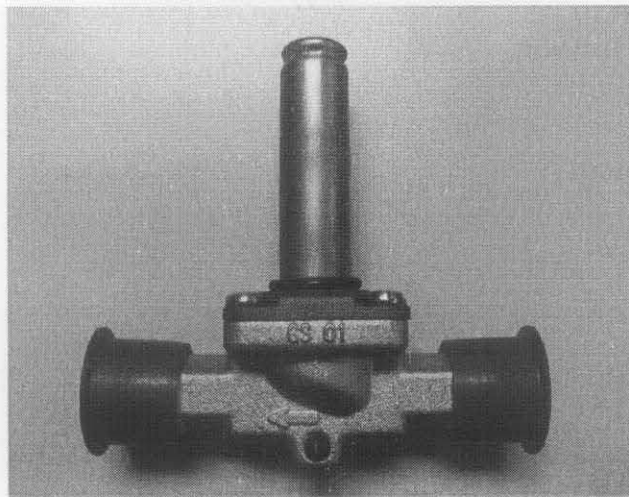


Figure 3.11: Solenoid valve



Figure 3.12: Check Valve

### 3.3.8 Other Components

Due to space constraints, most of the components of the system are placed on the outside of the indoor unit. As this is a test unit, such an arrangement is acceptable for preliminary feasibility tests. This will also allow easier change of EXV settings because the components are located outside. Figure 3.13 shows the piping and components on the outside of the indoor unit.

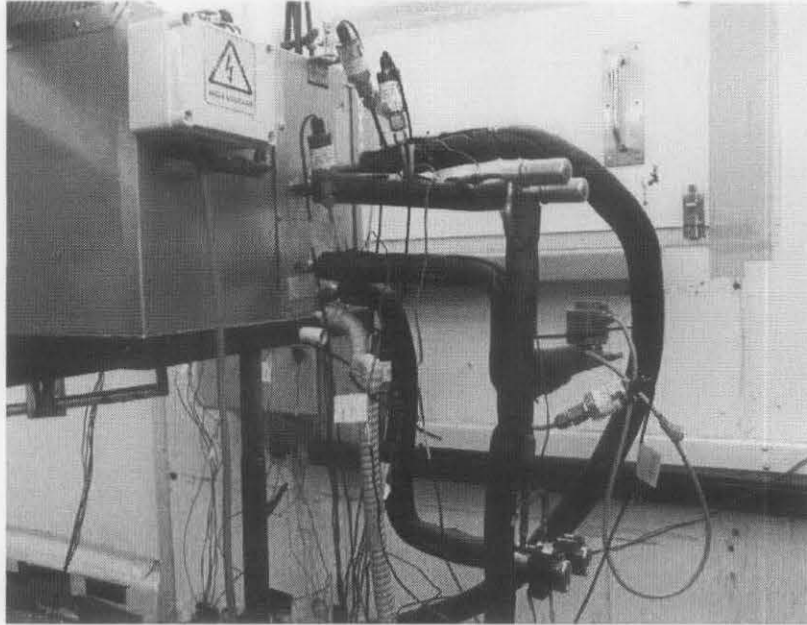


Figure 3.13: Piping and components of the evaporator-condenser system

### 3.4 Measuring Equipment

In this study, the temperatures along the refrigerant pipe circuit are measured by using Type-T thermocouples while the gauge pressures are measured by using Yokogawa FP201 pressure transmitters. The indoor unit entering and leaving dry-bulb and wet-bulb temperatures are taken by using air samplers which houses the RTDs. Pressure taps and thermocouples are placed on the compressor suction, compressor discharge, condenser inlet, condenser outlet, evaporator inlet, evaporator outlet, before EXV1, after EXV1, before EXV2, after EXV2, and reheat coil outlet.

The air flow rate of the indoor unit is measured with a nozzle chamber, which is designed in accordance with ASHRAE Standard 41.2 [41]. The nozzle chamber generally consists of a nozzle, blower, pressure tapplings and an inverter to control the blower motor. Figure 3.14 shows the schematic of the nozzle chamber.

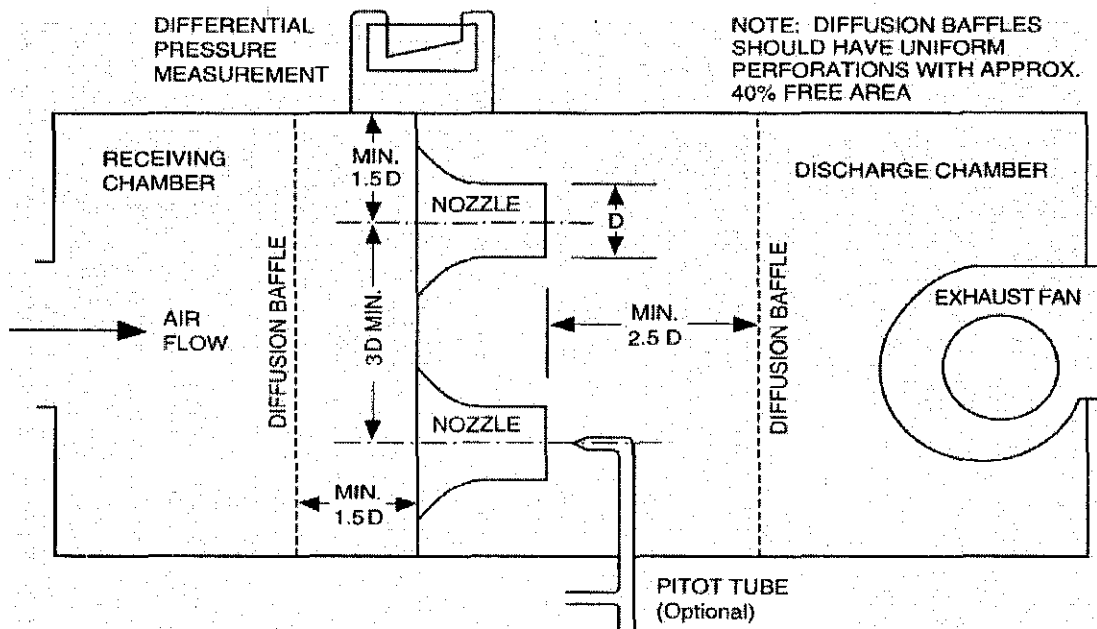


Figure 3.14: Schematic of the nozzle airflow measuring apparatus

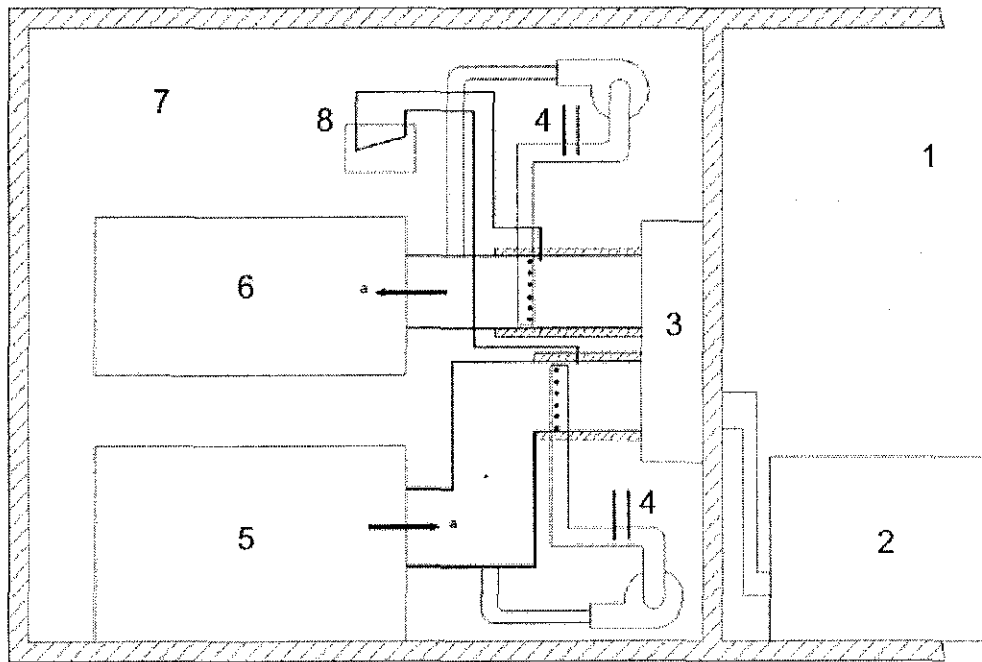
The psychrometric test room is designed in accordance with ISO standard 13253 [3] and ASHRAE Standard 37 [42]. The calculation method to determine the cooling performance of the unit is based on indoor test data using the loop air enthalpy test method. The room arrangement for the loop air enthalpy test method is shown in Figure 3.15.

The COP calculation for the experimental results is

$$\text{COP} = \frac{Q_{\text{total,air}}}{P_{\text{total}}} \quad (3 - 6)$$

$$P_{\text{total}} = P_{\text{comp}} + P_{\text{fan}} \quad (3 - 7)$$

Unlike equation 5 in section 3.2, the power input is redefined to include the fan power in addition to the compressor power. This is because Vapcyc is limited to only compressor power and fan power is not considered in the simulation.



**Key**

- |  |   |
|--|---|
| 1 outdoor-side test room                         | 5 reconditioning apparatus                        |
| 2 outdoor unit of equipment under test           | 6 air flow measuring apparatus                    |
| 3 indoor unit of equipment under test            | 7 indoor-side test room                           |
| 4 temperature and humidity measuring instruments | 8 apparatus for differential pressure measurement |
| <sup>a</sup> Airflow.                            |   |

Figure 3.15: Loop air enthalpy test method arrangement [41]



### 3.5 Experimental Methodology

This section explains the steps of performing the experimental study of the evaporator-condenser system.

#### 3.5.1 System Leak Check

Before the testing is performed, a system leak check is done to detect possible leaks due to improper brazing or other connections. Nitrogen gas is used to pressurize the system at approximately 2.8 MPa (400 psig) and the pressure readings are observed. The pressure readings will drop if there are any leaks in the system. Hence, all the joints at the system have to be checked individually using a soap solution. The soap solution is placed on the joint and observed. If bubbles form on the soap solution, it means that there is a leak in the system and the joint has to be repaired or replaced.

#### 3.5.2 Cooling System Refrigerant Optimization

The cooling system has to be optimized first before the reheat coil is tested. For this test, the solenoid valve is turned off to prevent refrigerant from entering the reheat coil. The optimization process takes place under ISO Standard Cooling condition.

The procedure to optimize the cooling system is as follows:

1. The cooling system is charged with 2.7 kg of R410A.
2. The system is turned on and the EXV is adjusted until the compressor discharge temperature is 75°C.
3. The system is run for 15 minutes to stabilize the readings.
4. The total capacity is noted.
5. Steps 3 and 4 are repeated with compressor discharge temperatures of 80°C and 85°C.

6. An additional 0.10 kg of R410a is charged into the cooling system and steps 2 to 5 are repeated.
7. Step 6 is repeated until there is a drop in performance compared to the previous charge weight.

The optimized charge will be the charge which gives the best performance at a certain compressor discharge temperature. This refrigerant charge and discharge temperature will be used for further tests.

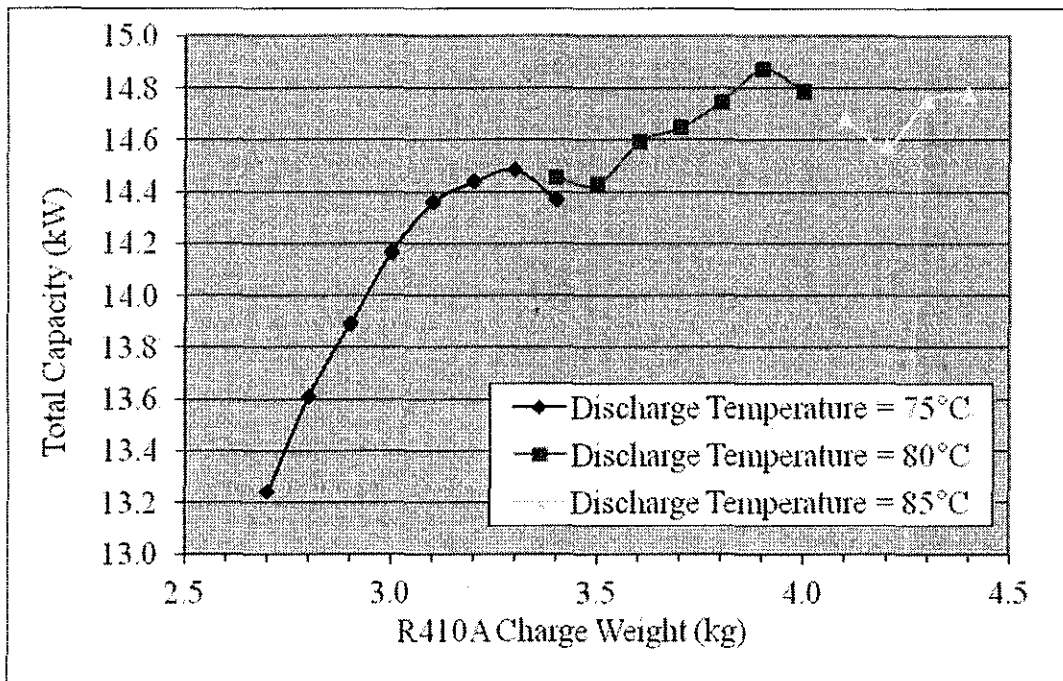


Figure 3.16: Charge optimization of YCC60C

Referring to Figure 3.16, the system is charged from 2.7 kg until 4.4 kg. For the testing with 75°C discharge temperature, the total capacity increases as the charge weight increases. At 3.3 kg charge weight, the total capacity reaches a peak, and drops off at 3.4 kg. Therefore, the testing is continued by changing the discharge temperature to 80°C and refrigerant is continued to be added. The total capacity again increases until it peaks at 3.9 kg and drops after that. The discharge temperature is increased to 85°C and refrigerant is added again. The highest capacity is at 80°C discharge temperature and 3.9 kg weight of R410a. Therefore, this charge weight is set as the optimum weight for this system.

The refrigerant in the system was recovered using a recovery machine. Then, 3.9 kg of refrigerant R410a is charged into the system and the test is repeated at 80°C discharge temperature. However, the suction superheat was on the low side, 3.7°C. A low superheat suction means that there is a chance for liquid refrigerant to enter the compressor, thereby reducing the reliability of the compressor. To increase the superheat temperature, the discharge temperature is raised to 85°C. The resultant superheat at suction was 7.8°C, which resulted in a relatively small sacrifice in performance (0.39% lower). Therefore, the discharge temperature for the following tests was maintained as 85°C. The difference in performance for the two discharge temperatures is shown in Table 3.2.

Table 3.2: Performance at 80°C and 85°C discharge temperature

|  | $T_d = 80^\circ\text{C}$ | $T_d = 85^\circ\text{C}$ |
|--|--------------------------|--------------------------|
| Temp Comp Discharge ( $^\circ\text{C}$ ) | 80.1                     | 84.6                     |
| Total Capacity (kW)                      | 15.06                    | 15.00                    |
| Superheat Suction ( $^\circ\text{C}$ )   | 3.7                      | 7.8                      |
| Subcooling ( $^\circ\text{C}$ )          | 7.5                      | 7.8                      |

The experimental data used to plot charge optimization is shown in Appendix A.

### 3.5.3 Humidity Control System Test

Having determined the optimum charge for the cooling system, the refrigerant is released from the system. After that, the system is evacuated and purged with R410a. Now the predetermined optimum charge weight of R410a is filled into the system. The cooling system is then operated again to re-confirm the performance of the system. This will become the benchmark for future tests of the humidity control system.

There are many parameters that can be adjusted in the air conditioning system, viz., condensing pressure, evaporating pressure, discharge temperature, refrigerant charge and air flow. A variation in each of these parameters affects all the others. For example, lowering the condensing pressure will result in a lower evaporating pressure. With all these parameters to consider, certain inputs will be unchanged for the test. This is to consider a simpler test method for data collection. Among the parameters held constant are:

1. Compressor discharge temperature
2. Indoor and outdoor air temperatures
3. Refrigerant charge
4. Air flow rate

To test for the effect of the reheat coil in the system, a reheat EXV is used to expand the refrigerant entering the reheat coil to a pre-determined temperature. However, this temperature must be higher than the air temperature leaving the evaporator to ensure that the air is reheated. Therefore, a range of 20°C to 45°C is used as a guideline to control the reheat EXV.

#### *3.5.4 Measurement Uncertainty*

Uncertainties in the experimental measurement data were calculated using the error propagation method by Kline and McClintok [43].

The uncertainty analysis for air conditioner cooling capacity using air-enthalpy method was carried out as per Jia et al. [44].

Table 3.3 lists the measurement instruments used in the experiment and their respective uncertainties. In calculating the uncertainties, expressed as algebraic

combination of several variables A, B and C, the relationships shown in Table 3.4 have been used.

The calculated expanded uncertainties from the experimental data for a 95% confidence level are as follows:

- a) Total capacity:  $\pm 2.4\%$
- b) Sensible capacity:  $\pm 3.2\%$
- c) Latent capacity:  $\pm 8.3\%$

Table 3.3: List of uncertainties of measurement instruments

| Instrument                      | Uncertainty                       |
|---------------------------------|-----------------------------------|
| RTD temperature sensor          | $\pm 0.03^\circ\text{C}$          |
| Differential pressure manometer | $\pm 0.05 \text{ mm H}_2\text{O}$ |
| Power meter                     | $\pm 0.7 \text{ W}$               |

Table 3.4: Error propagation relationship

| No. | Relation between Z and (A,B,C) | Relation between $\Delta Z$ and ( $\Delta A, \Delta B, \Delta C$ )  |
|-----|--------------------------------|---|
| 1   | $Z = A \pm B \pm C$            | $(\Delta Z)^2 = (\Delta A)^2 + (\Delta B)^2 + (\Delta C)^2$   |
| 2   | $Z = A * \frac{B}{C}$          | $\left(\frac{\Delta Z}{Z}\right)^2 = \left(\frac{\Delta A}{A}\right)^2 + \left(\frac{\Delta B}{B}\right)^2 + \left(\frac{\Delta C}{C}\right)^2$ |
| 4   | $Z = \ln A$                    | $\Delta Z = \frac{\Delta A}{A}$   |
| 8   | $Z = A^n$                      | $\Delta Z = Zn \left(\frac{\Delta A}{A}\right)$   |

### **3.6 Chapter Summary**

This chapter begins by describing the circuit design of the evaporator-condenser system. Then, the simulation method using Vapcyc and CoilDesigner to determine the performance of the evaporator-condenser system is shown. The experimental setup and test procedures are described. The optimum refrigerant R410a weight to be used in the experiment is found to be 3.9 kg. Finally, the uncertainties in measurement are determined.

## CHAPTER IV

### RESULTS AND DISCUSSION

#### 4.0 Chapter Overview

This chapter presents the results of the simulation and numerous tests that have been performed. A comparison study is done between test results and simulation results which were described in the previous chapter. The system curve is also plotted on a P-h diagram to illustrate the differences of the evaporator-condenser system compared to the conventional system.

The data used to plot the reheat circuit experimental results are given in Appendix C. The calculation method used to determine the refrigerant mass flow rate and the results are given in Appendix D.

A summary of the equations used in Chapters III and IV are shown in Appendix E.

#### 4.1 Implications of the Balancing Simulation

The results of the evaporator-condenser simulation are summarized in Table 4.1. The conditions of air entering the evaporator-condenser follows ISO standard conditions i.e. 27°C dry bulb temperature and 19°C wet bulb temperature [3]. The reduction in relative humidity shows that the evaporator-condenser system is able to perform enhanced dehumidification compared to the conventional system. The cooling capacity has increased compared to the conventional system by 9.11% but needs 1.06% higher compressor work. Overall, the COP is higher by 7.96%.



Table 4.1: Simulation Results

|                                     |       | Without Reheat |         | With Reheat |         |
|-------------------------------------|-------|----------------|---------|-------------|---------|
| <b>Air Side</b>                     |       | Entering       | Leaving | Entering    | Leaving |
| Air Dry Bulb Temperature            | °C    | 27.00          | 12.91   | 27.00       | 12.90   |
| Air Wet Bulb Temperature            | °C    | 19.00          | 12.88   | 19.00       | 12.26   |
| Relative Humidity                   | %     | 46.95          | 99.73   | 46.95       | 93.13   |
| Enthalpy                            | kJ/kg | 53.81          | 36.34   | 53.81       | 34.74   |
| Air-Side Capacity                   | kW    | 13.34          |         | 14.56       |         |
| <b>Compressor Power Calculation</b> |       |                |         |             |         |
| Suction Temperature                 | °C    | 12.56          |         | 11.73       |         |
| Suction Pressure                    | MPa   | 1.05           |         | 1.04        |         |
| Suction Enthalpy                    | kJ/kg | 428.05         |         | 427.49      |         |
| Discharge Temperature               | °C    | 88.48          |         | 88.48       |         |
| Discharge Pressure                  | MPa   | 3.11           |         | 3.11        |         |
| Discharge Enthalpy                  | kJ/kg | 480.44         |         | 480.44      |         |
| Enthalpy Difference                 | kJ/kg | 52.39          |         | 52.95       |         |
| Refrigerant Mass Flow Rate          | kg/hr | 357.66         |         | 357.66      |         |
| Calculated Power                    | kW    | 5.20           |         | 5.26        |         |
| COP                                 | W/W   | 2.56           |         | 2.77        |         |

While the evaporating temperature is indeed lowered when simulating the evaporator-condenser performance, the refrigerant mass flow rate remains unchanged during the simulation process. A consequence of the lower evaporating temperature is higher moisture removal rate by the evaporator, as discussed in Chapter 2. Furthermore, at a lower evaporating temperature the COP for the system should also be lower. This does not appear to be the case in the simulation.

The results of the balancing simulation using Vapcyc are shown in Appendix B.

#### **4.2 Performance and Moisture Removal**

As shown in Figure 4.1, there is a decrease in total capacity and absolute humidity of the air leaving with higher reheat coil entry temperatures. The maximum reduction in absolute humidity of the air leaving is approximately 9.90% as compared with no reheat coil. This occurred at the reheat coil entry temperature of 43.0°C. A poorer cooling performance would usually result in less moisture removal, therefore resulting in a higher absolute humidity. In this case, the absolute humidity is also lowered as the reheat coil entry temperature increases. Therefore, this phenomenon has to be considered from a different perspective to understand the reason.

Although the discharge temperature is maintained at 85°C, the evaporator saturation temperature is different for each test. A low evaporating temperature results in low capacity and therefore, the cooling capacity of the cycle with the reheat coil is lower compared to the one without it. As the reheat coil entry temperature increases, the evaporating temperature decreases as shown in Figure 4.2. This explains the performance loss of the system. To understand why the absolute humidity is lower when the total capacity is lower, the data is analyzed in terms of latent heat and sensible heat.

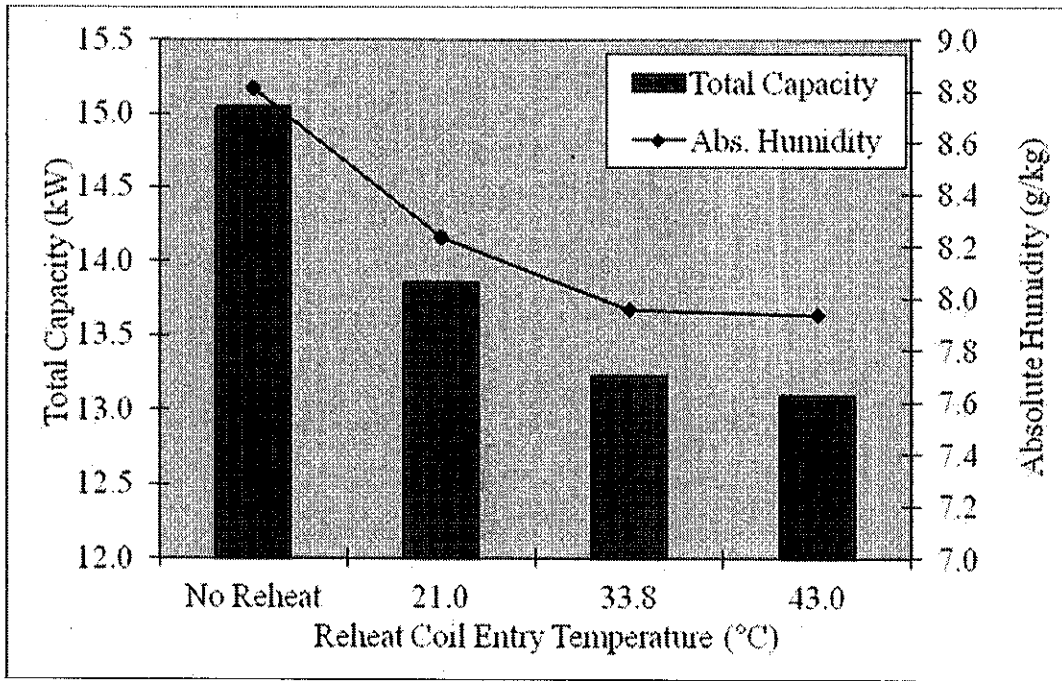


Figure 4.1: Effect of reheat coil entry temperature on total capacity and absolute humidity

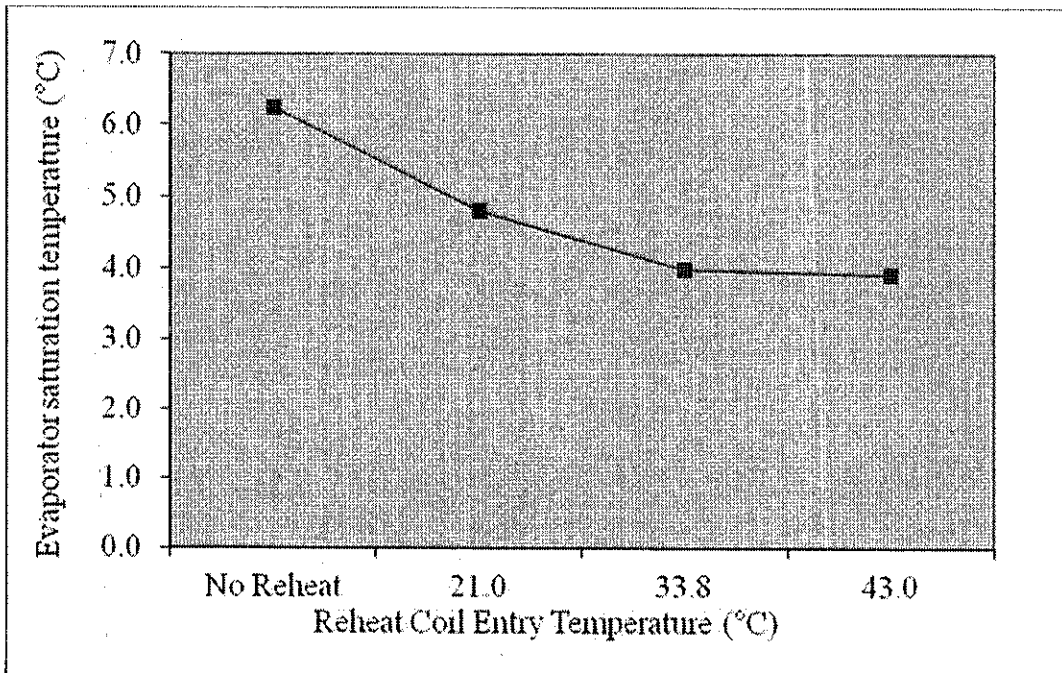


Figure 4.2: Evaporator saturation temperature against reheat coil entry temperature

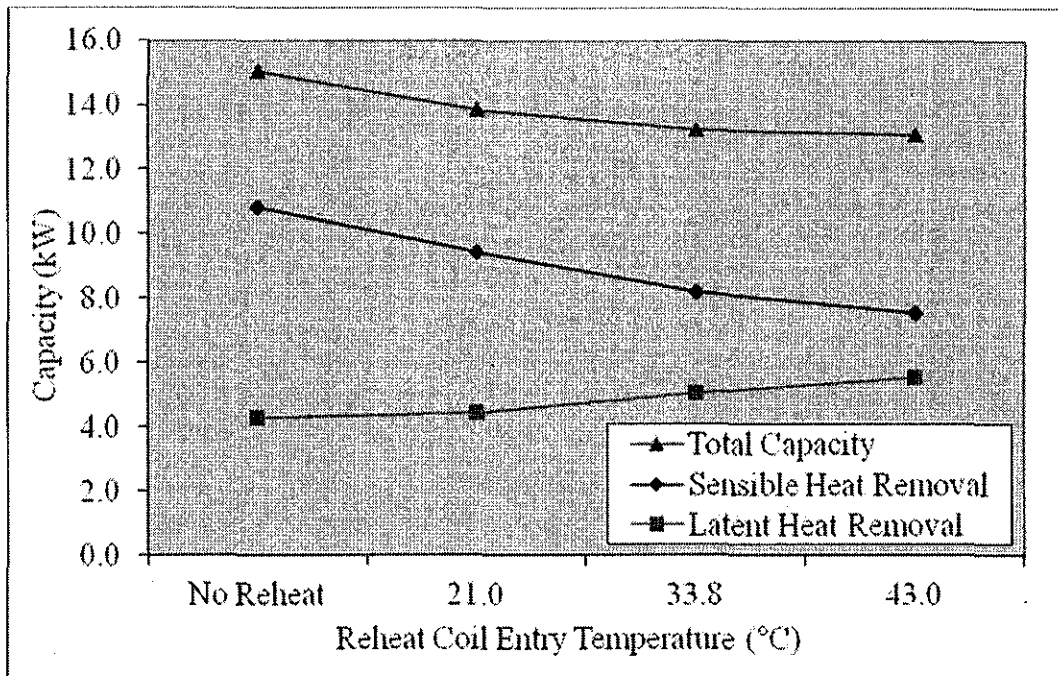


Figure 4.3: Sensible and latent heat removal

Due to the performance loss in the system with reheat, it is expected that the moisture removal would be less than that without reheat. However, the test results show that the absolute humidity is lower with the reheat coil, which suggests that the moisture removal has increased. By comparing the removal of latent heat and sensible heat at different reheat coil entry temperatures as shown in Figure 4.3, it is seen that although the total capacity is decreasing, the latent heat removal is increasing. The total capacity is reduced by 7.9%, 12.1% and 12.9% for reheat coil entry temperatures of 21.0°C, 33.8°C and 43.0°C respectively. The sensible heat is reduced by 12.7%, 28.2% and 30.1% while the latent heat is improved by 4.2%, 28.6% and 30.3% for reheat coil entry temperatures of 21.0°C, 33.8°C and 43.0°C respectively. A higher value of latent heat removal implies that more moisture is being removed from the air.

### 4.3 Coefficient of Performance

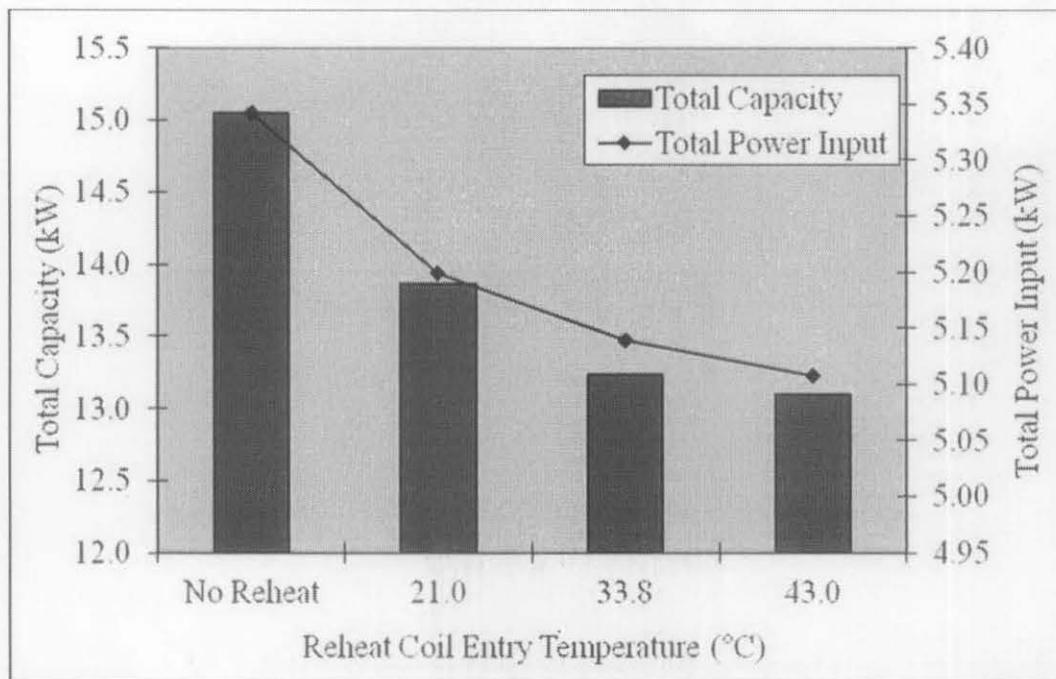


Figure 4.4: Total capacity and power input against reheat coil entry temperature

Figure 4.4 shows the total capacity and the power input of the evaporator-condenser system at different reheat coil entry temperatures. Generally, the power consumption is lower as the total capacity decreases. However, the percentage change of the reduction in total capacity is higher compared with the reduction in power consumption. Therefore, the COP is lower for a system with the reheat coil.

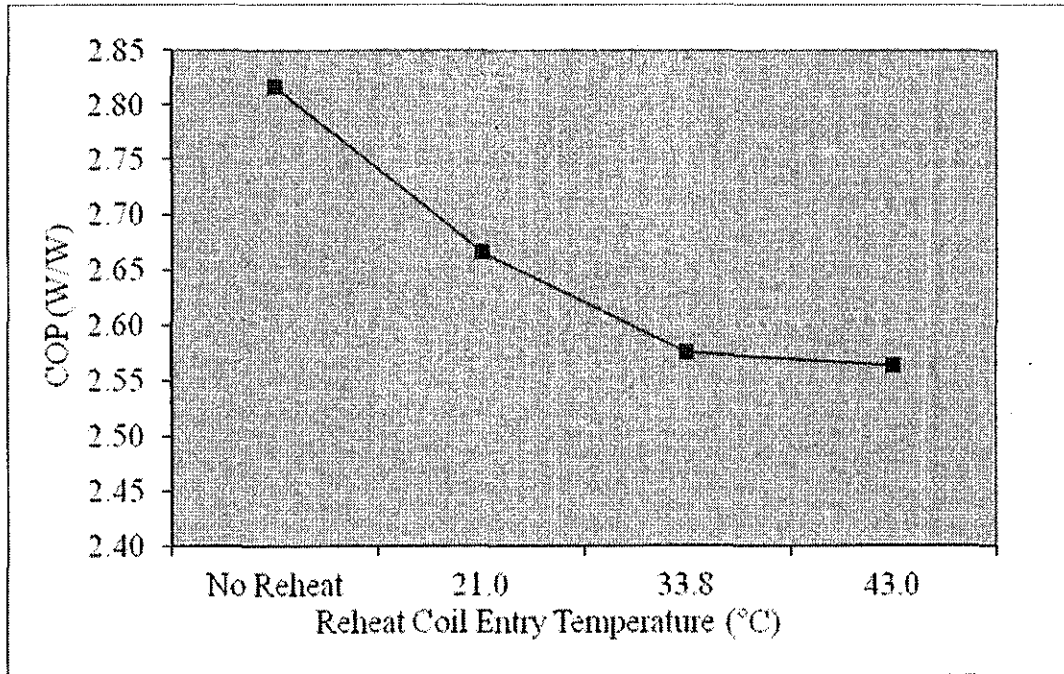


Figure 4.5: Coefficient of performance against reheat coil entry temperature

Figure 4.5 shows the COP at different reheat coil entry temperatures. As expected, the COP is lower as the reheat coil entry temperature increases due to the lower total capacity of the system.

#### 4.4 Relative Humidity

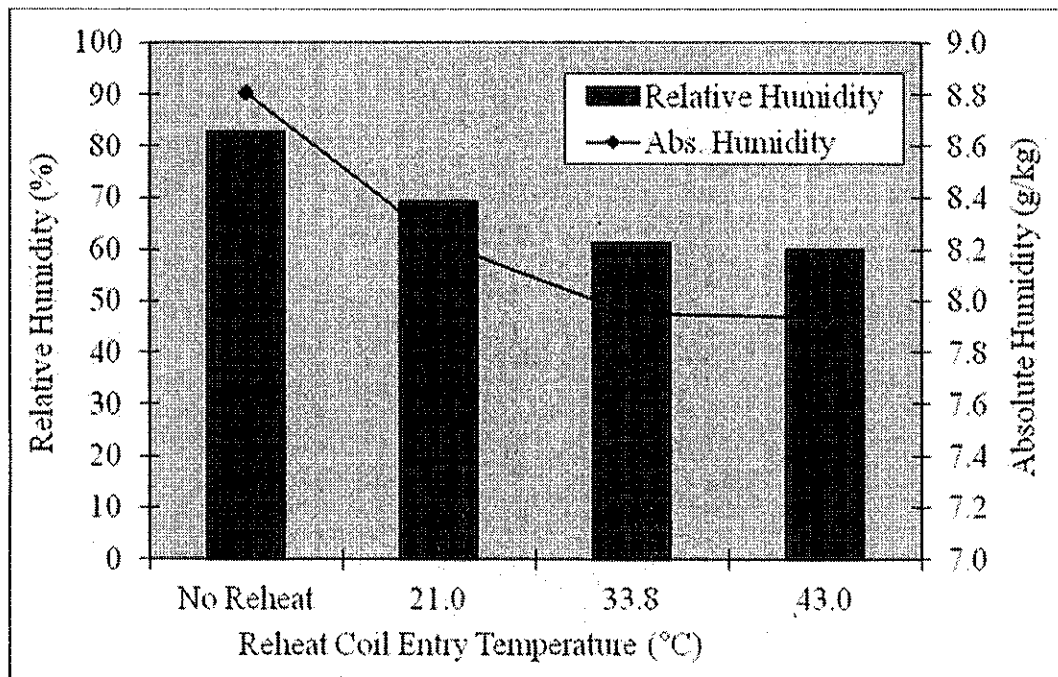


Figure 4.6: Effect of entering reheat coil temperature on relative humidity

Figure 4.6 shows the relationship between the reheat coil entry temperature and the relative humidity of the air leaving. The relative humidity is lower as the reheat coil entry temperature increases. This is because the absolute humidity of the air leaving is lower due to the additional moisture removal by the evaporator coils. As explained in the previous section, this is due to the higher latent heat removal with the reheat coil.

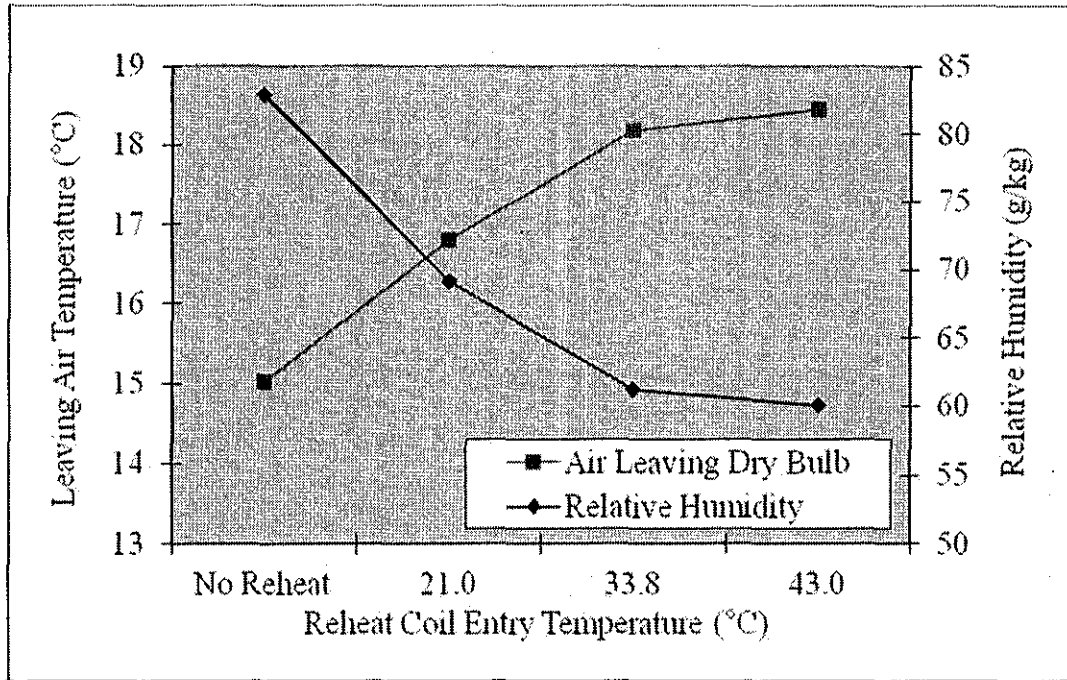


Figure 4.7: Air leaving dry bulb temperature

The leaving air dry bulb temperature is also higher compared to the case without reheat as shown in Figure 4.7. As the dry bulb temperature increases, the maximum amount of moisture the air can hold increases. Therefore, the relative humidity decreases at a specific absolute humidity as the air temperature rises.



#### 4.5 Comparing Simulation Results and Test Results

Preliminary simulation results suggested that the method of using evaporator-condenser systems is able to provide an increase in cooling performance and also enhancement in moisture removal. However, as evident in the test results, the cooling performance was poorer with the reheat coil.

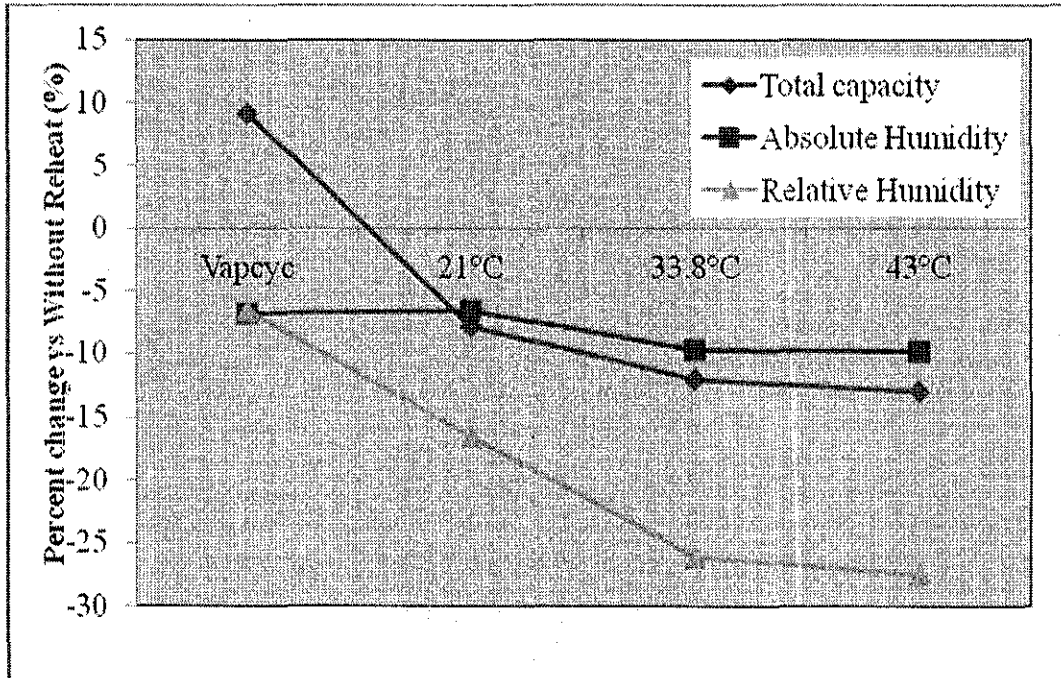


Figure 4.8: Simulation and test comparisons

Figure 4.8 shows the comparisons between simulation and test results. As shown in Table 4.1, the simulation total capacity is 9.11% better with the reheat coil while the absolute humidity and relative humidity are lower by 6.8% and 6.6% respectively. The experimental results presented in the above figure show that the total capacity, absolute humidity and relative humidity decrease as the reheat coil temperature increases. Instead of the simulated increase in total capacity, the tested total capacity is lower compared to the system without reheat. The tested relative humidity value is much lower than simulated value.

Table 4.2 shows the system performance of the evaporator-condenser system at different reheat coil entry temperatures.

Table 4.2 System performance of the evaporator-condenser system

| Reheat coil entry temperature | Change compared to system with reheat (%) |                   |                   |
|-------------------------------|---|-------------------|-------------------|
|                               | Total capacity                            | Absolute humidity | Relative humidity |
| 21°C                          | -7.9                                      | -6.6              | -16.5             |
| 33.8°C                        | -12.1                                     | -9.7              | -26.1             |
| 43°C                          | -13.0                                     | -9.9              | -27.5             |

A possible explanation for the disagreement between simulation and experiments may be stated as follows:

Vapcyc and CoilDesigner were designed to be used with conventional air conditioning systems. It is concluded that they are not adequate and do not have the flexibility for analyzing the evaporator-condenser system that is considered here. Due to the limitations of the Vapcyc to simulate the evaporator-condenser system, it was necessary to make certain assumptions. That is another possible reason for the discrepancy.

#### 4.5.1 Refrigerant Mass Flow Rate

One of the causes of this variation is the refrigerant mass flow rate. To simplify the simulation, the refrigerant mass flow rate was assumed equal for both systems with and without the reheat coil. However, with the addition of the reheat coil and its EXV, the internal resistance of the system has increased. This causes a reduction in refrigerant mass flow rate which in turn, will reduce the cooling performance. The mass flow rate of the system can be estimated as follows:

$$Q_{\text{total,air}} = Q_{\text{total,ref}} \times \eta \quad (4 - 1)$$

where

$$\eta = 0.95 \text{ (By assuming 5\% heat transfer losses between air-side and refrigerant-side)}$$

The refrigerant flow rate is then calculated by using the following equation:

$$Q_{\text{ref}} = \dot{m}_{\text{ref}} \times \Delta h_{\text{ref, evap}} \quad (4 - 2)$$

where

$$\Delta h_{\text{ref, evap}} = h_{\text{evap, outlet}} - h_{\text{evap, inlet}} \quad (4 - 3)$$

The enthalpy difference of the refrigerant is taken to be the difference between the enthalpies at inlet and outlet pipes of the evaporator. However, the enthalpy at the Evaporator inlet is difficult to measure because of the refrigerant quality which could not be measured directly in the experiment. To overcome this problem, it is assumed that the refrigerant leaving the condenser has the same enthalpy as at the evaporator inlet. The expansion process of the refrigerant is assumed to be adiabatic.

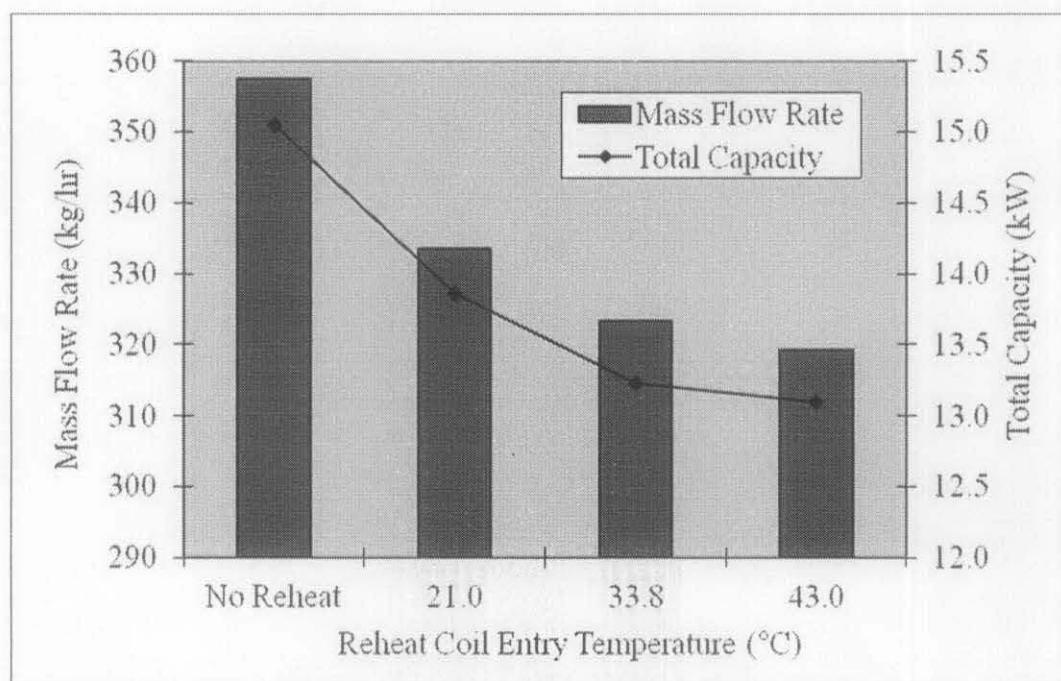


Figure 4.9: Refrigerant mass flow rate

From Figure 4.9, it is clear that as the reheat coil entry temperature increases, the mass flow rate reduces and correspondingly, the total capacity also decreases. A higher reheat coil entry temperature implies that the expansion of the refrigerant is lower. The refrigerant expansion is achieved by opening or closing the EXV suitably until the required refrigerant temperature/pressure is reached. With a fixed compressor power, the extra pressure drop in the EXV and the additional reheat coil cause lower refrigerant mass flow rate. In contrast, Vapcyc fixes the mass flow rate

based on the compressor characteristics, superheat and subcool by means of a built-in algorithm.

In order to achieve a higher cooling performance, an increase in the refrigerant mass flow rate is to be considered. One method to increase the refrigerant mass flow rate is to lower the compressor discharge temperature from 85°C. The disadvantage of lowering the discharge temperature is that it will cause the evaporator superheat to decrease, allowing liquid refrigerant to return to the compressor. Presence of liquid at the compressor suction can lead to compressor reliability problems. Another way to increase the mass flow rate is to use a compressor of higher output, resulting in an increase in initial and operating costs.

The calculation of mass flow rates of the system at different reheat temperatures is summarized in Appendix C.

#### *4.5.2 System Pressures*

In the simulation, the evaporating and condensing temperatures are assumed to be invariant. Under actual testing conditions, the evaporating and condensing temperatures are dependent on each other. If the evaporating temperature decreases, the condensing temperature also decreases and vice versa. This is because the compression ratio of the compressor is a fixed value and cannot be changed. The changes in suction and discharge pressures at different reheat coil entry temperatures can be seen in Figure 4.10. The suction and discharge pressures are used to represent the system pressures.

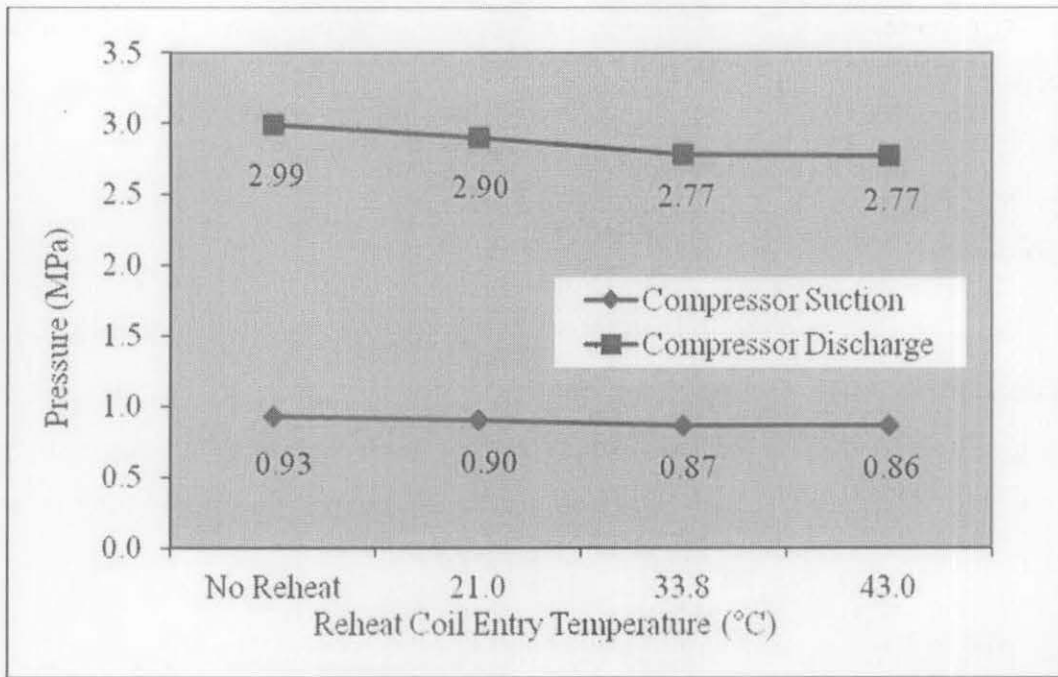


Figure 4.10: Suction and discharge pressures

#### 4.6 P-h Diagram Comparison

Figure 4.11 shows the reheat system plotted on a P-h diagram for three different reheat coil entry temperatures compared against the conventional benchmark cooling system.

The reheat system indeed lowers the quality of refrigerant at the inlet to the evaporator, so increasing the refrigerant enthalpy difference. This is represented by the longer evaporator red line from points A to B on the P-h diagrams. As hypothesized in Section 3.1, the increase in enthalpy difference will result in a higher cooling performance. However, as discussed in Section 4.4, the mass flow rate is more dominant than the enthalpy difference in determining the cooling performance. The P-h diagram is only able to illustrate the enthalpy difference, but by itself is not sufficient to determine the total capacity.

When the reheat coil entry temperature is 21.0°C, the condenser pressure difference between the “cooling only” system and the “cooling and reheat system” is relatively small as compared to reheat coil entry temperatures of 33.8°C and 43.0°C.

It is interesting to note that as the reheat coil entry temperature increases, the condensing temperature for the “cooling and reheat” system reduces. This is because of the testing condition where the discharge temperature is maintained at 85°C by adjusting the cooling coil EXV. Due to this criterion, the P-h graph appears to shift downwards as the reheat coil entry temperature increases.

Figures 4.11A, 4.11B and 4.11C refer to the P-h diagram for reheat coil temperatures of 21.0°C, 33.8°C and 43.0°C respectively.

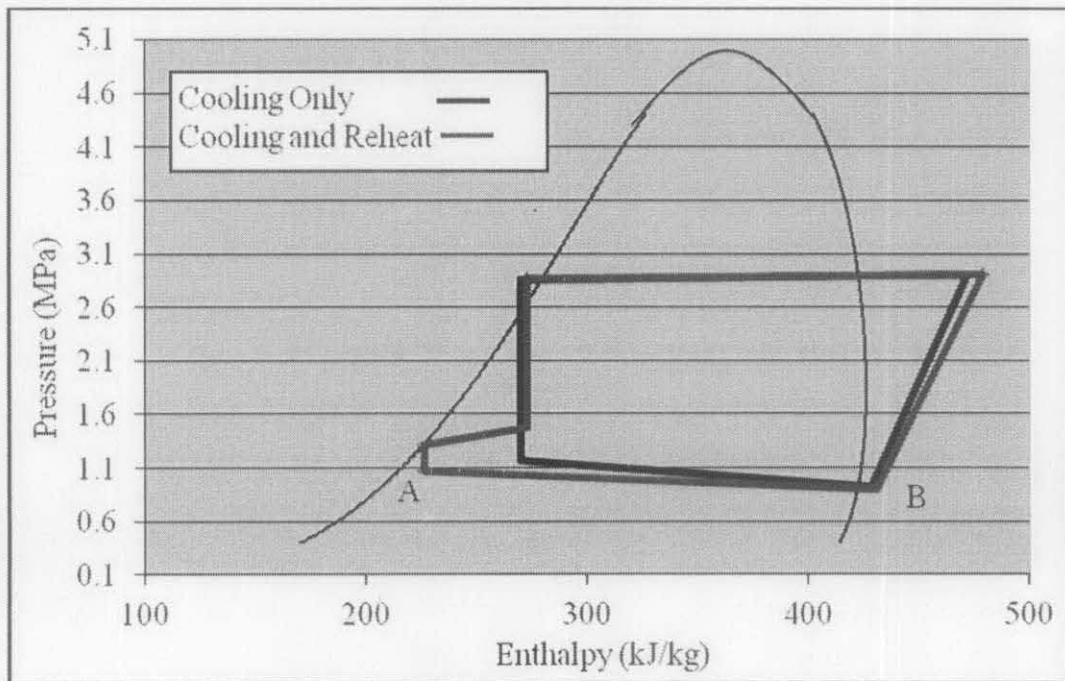


Figure 4.11A: P-h diagram for reheat coil entry temperature of 21.0°C

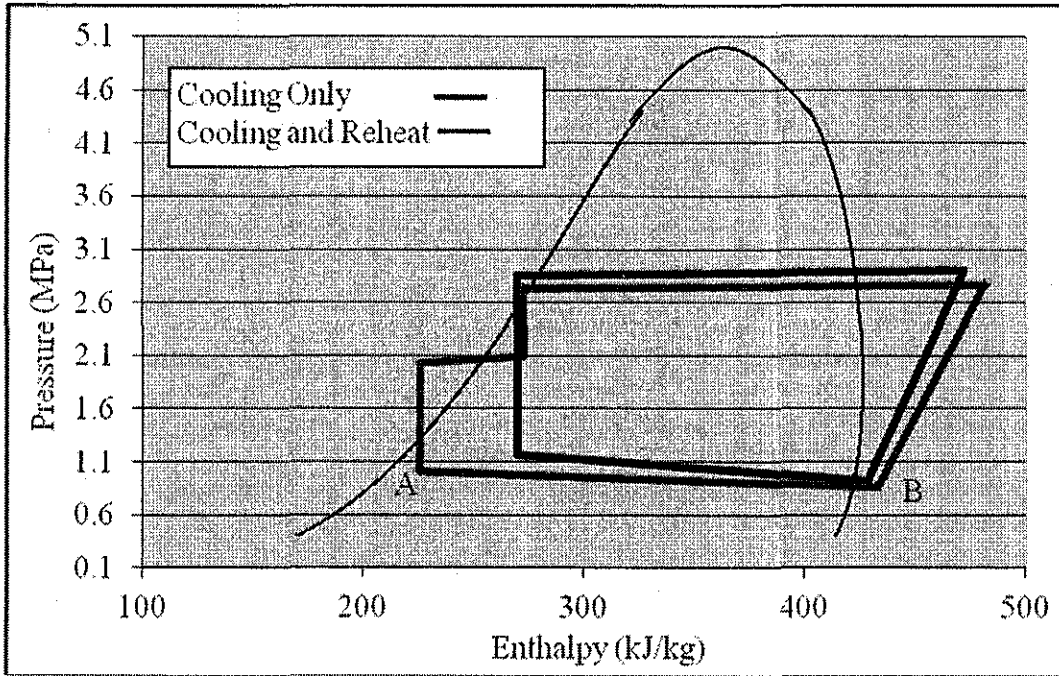


Figure 4.11B: P-h diagram for reheat coil entry temperature of 33.8°C

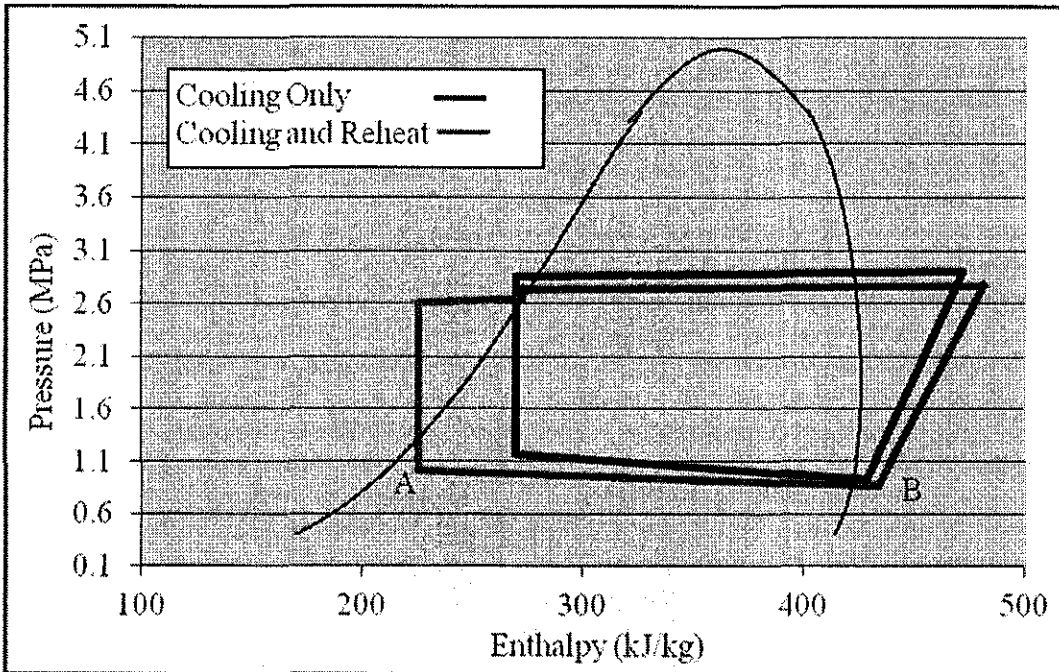


Figure 4.11C: P-h diagram for reheat coil entry temperature of 43.0°C

## 4.7 System Comparisons

The proposed evaporator-condenser system is similar to the thermosyphon heat exchanger (THX) and desiccant wheel system because of the reheat of air after the cooling coils. Therefore, it is appropriate to draw a comparison between the present results of the evaporator-condenser system with those of the THX and desiccant wheel systems.

The experimental results of the evaporator-condenser system show that there is a drop in cooling performance while improving the moisture removal and lowering the relative humidity. The results shown in Table 4.2 follow the trends obtained in the experiment using desiccant wheel for humidity control performed by Subramanyam et al. [19] who reported that the COP of the desiccant wheel system was lowered by 5% while the moisture removal rate was improved as shown in Figure 4.12. The reason for the lower COP is because of the lower cooling performance. Furthermore, an experimental study on a THX system by the author [45] also shows a similar trend, where the COP was reduced by 3.78% using the THX system. The relative humidity was lower with the THX system compared to the conventional system as shown in Figure 4.13. While all systems are able to improve the moisture removal, the cooling performance is invariably poorer.

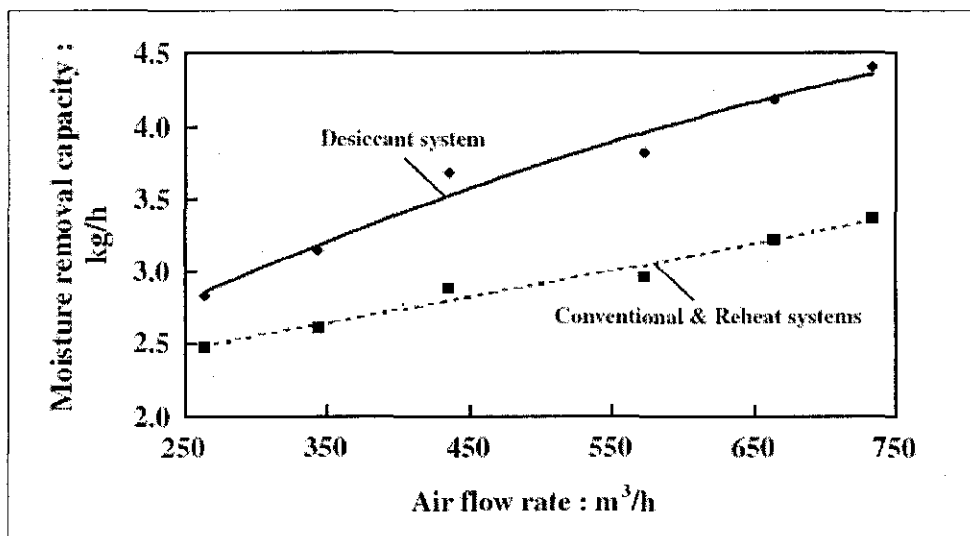


Figure 4.12: Variation of moisture removal capacity with air flow rate (Desiccant wheel) [19]



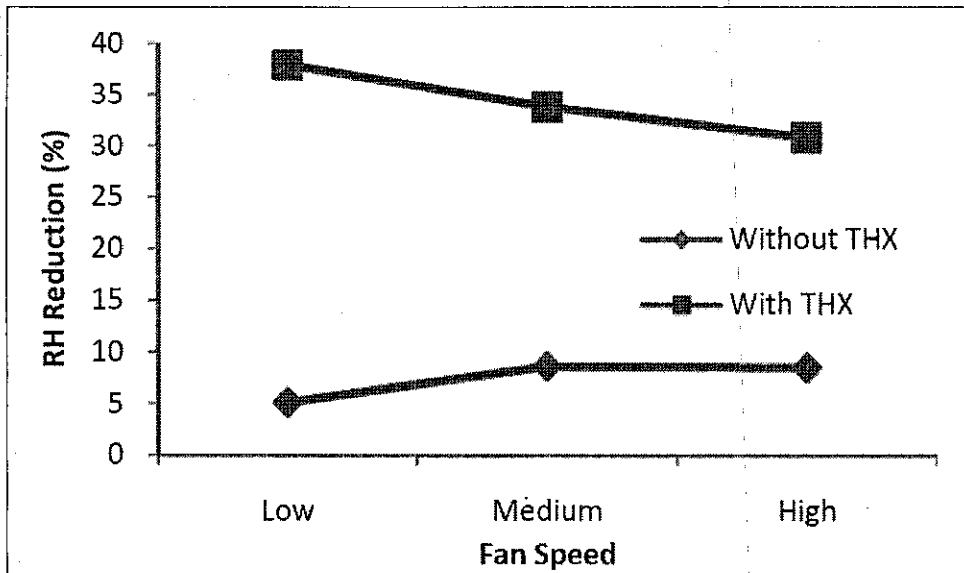


Figure 4.13: RH reduction vs fan speed (THX) [44]

Several advantages are present in the evaporator-condenser system as compared to the THX and desiccant wheel systems. The amount of space required to install a desiccant wheel system or THX is quite large as compared to the evaporator-condenser system. This is because the size of the desiccant wheel and the THX are both larger compared to just adding a reheat coil to the existing cooling system. Furthermore, the use of an EXV to control the refrigerant temperature of the reheat coil provides a better method for varying the required amount of moisture removal. While it is possible to control the moisture removal rate in desiccant wheel and heat pipe systems by means of by-pass air, major modifications have to be made to the system layout. The use of the evaporator-condenser system proves advantageous with its relative simplicity, ability to control humidity and smaller floor space required for installation.

## **4.8 Chapter Summary**

The results of the Vapcyc and CoilDesigner simulation and the experiment were presented in this chapter. Comparisons between the simulation and experimental results were done and the reasons for the differences were given. Finally, the evaporator-condenser system was compared with the THX system and desiccant wheel system. A similar trend was observed in all the systems whereby the total capacity was lower while the moisture removal was higher.

## CHAPTER V

### CONCLUSIONS

#### 5.1 Conclusions

An experimental study has been performed on an evaporator-condenser system in an attempt to enhance air dehumidification using a constant speed compressor and fixed air volume.

The results show that the moisture removal rate using the evaporator-condenser system has improved by 6.3% to 9.9% depending on the reheat coil entry temperature of refrigerant. The higher latent heat removal contributes to a higher rate of moisture removal. The cooling performance is reduced by 7.90% to 12.98% depending on the reheat coil entry temperature of refrigerant. The results are similar to those of the thermosyphon heat exchanger system and desiccant wheel system.

A comparison between the evaporator-condenser, desiccant wheel and loop heat pipe systems has been made. While all systems are able to enhance moisture removal, the evaporator-condenser system is advantageous in its simplicity, floor space and method of controlling the moisture removal rate.

Generally, the cooling performance will decrease as the reheat coil temperature increases. At the same time, the moisture removal is enhanced as the reheat coil temperature increases. The concomitant benefits are a more comfortable environment, better productivity and more healthy conditions.

## **5.2 Recommendations**

- A. The evaporating temperature is an important aspect in the air conditioning system when determining the performance. Therefore, the temperature should be maintained by adjusting the EXV opening instead of maintaining the discharge temperature.
- B. The available software is not suitable for simulating evaporator-condenser systems for humidity control. Further studies should be conducted to produce an advanced algorithm to simulate the evaporator-condenser system.

## REFERENCES

- [1] Y.A. Cengel, M.A. Boles. *Thermodynamics: An Engineering Approach – Fourth Edition*. McGraw Hill, New York, 2002.
- [2] ASHRAE. “ASHRAE Standard 55 - Thermal Environmental Conditions for Human Occupancy” Atlanta, GA, USA, 2004.
- [3] ISO. “ISO Standard 13253 Ducted air-conditioners and air-to-air heat pumps - Testing and rating for performance” Geneva, Switzerland, 2011.
- [4] C.M. Chu , T.L. Jong, Y.W. Huang. “Thermal comfort control on multi-room fan coil unit system using LEE-based fuzzy logic”, *Energy Conversion and Management* 46 (9–10), pp. 1579–1593, 2005.
- [5] J. Liang, R. Du. “Design of intelligent comfort control system with human learning and minimum power control strategies”, *Energy Conversion and Management* 49 (4), pp. 517–528, 2008.
- [6] R.Z. Freire, G.H.C. Oliveria, N. Mendes. “Predictive controllers for thermal comfort optimization and energy savings”, *Energy and Buildings* 40 (7), pp. 1353–1365, 2008.
- [7] P.O. Fanger. *Thermal comfort: analysis and applications in environmental engineering*. Danish Technical Press, Copenhagen, 1970
- [8] P.O. Fanger. *Thermal Comfort*. Robert E. Krieger Publishing Company, Malabar, FL, 1982.
- [9] K.H. Yang, C.H. Su. “An approach to building energy savings using the PMV index”, *Building and Environment* 32 (1), pp. 25–30, 1997.

- [10] S. Kumar, A. Mahdavi. "Integrating thermal comfort field data analysis in a case-based building simulation environment" *Building and Environment* 36 (6), pp. 711–720, 2001.
- [11] J. Han, G.Q. Zhang, Q. Zhang, J.W. Zhang, J.L. Liu, L.W. Tian, C. Zheng, J.H. Hao, J.P. Lin, Y.H. Liu, D.J. Moschandreas. "Field study on occupants' thermal comfort and residential thermal environment in a hot-humid climate of China", *Building and Environment* 42 (12), pp. 4043–4050, 2007.
- [12] A.I. Stamou, I. Katsiris, A. Schaelin. "Evaluation of thermal comfort in Galatsi Arena of the Olympics "Athens 2004" using a CFD model", *Applied Thermal Engineering* 28 (10), pp. 1206–1215, 2008.
- [13] A.A. Chowdhury, M.G. Rasul, M.M.K. Khan. "Thermal-comfort analysis and simulation for various low-energy cooling-technologies applied to an office building in subtropical climate", *Applied Energy* 85 (6), pp. 449–462, 2008.
- [14] P.N. Ananthanarayanan. *Basic Refrigeration and Air Conditioning 3rd Edition*. Tata McGraw-Hill, New Delhi, 2005.
- [15] H.R. Trechsel. *Moisture Control in Buildings*. American Society for Testing and Materials, Philadelphia, 1994.
- [16] D. Bearg. "Indoor air quality and humidity control", *Air-conditioning, Heating and Refrigeration News*, 1992.
- [17] N. Petchers. *Combined Heating, Cooling and Power Handbook: Technologies and Applications*. The Fairmount Press, Georgia, 2003.
- [18] ASHRAE. "Handbook—HVAC Systems and Equipment", American Society of Heating, Refrigeration and Air-conditioning Engineers, Atlanta, GA, USA, 2008.
- [19] N. Subramanyam, M.P. Maiya, S.S. Murthy. "Application of desiccant wheel to control humidity in air-conditioning systems", *Applied Thermal Engineering* 24, pp. 2777-2788, 2004.

- [20] B.L. Capehart, W.C. Turner, W.J. Kennedy. *Guide to Energy Management Fourth Edition*. The Fairmount Press. Georgia, 2003.
- [21] P.W. Xiao, P. Johnson, A. Akbarzadeh. "Application of Heat Pipe Heat Exchangers to Humidity Control in Air Conditioning Systems" *Applied Thermal Engineering Vol 17 No 6*, pp. 561-568, 1997.
- [22] M.K. Khattar, S.M. Ramanan. "Fan cycling effects on air conditioner moisture removal performance in warm, humid climates" Presented at the international symposium on moisture and humidity, April, Washington, DC, 1985.
- [23] H.I. Henderson. "An experimental investigation of the effects of wet and dry coil conditions on cyclic performance in the SEER procedure" *In Proceedings of USNC/IIR refrigeration conference at Purdue University*, 1990, IN. West Lafayette.
- [24] X.G. Xu, S.M. Deng, M.Y. Chan. "A new control algorithm for direct expansion air conditioning systems for improved indoor humidity control and energy efficiency" *Energy Conversion and Management 49*, pp. 578-586, 2008.
- [25] K.J. Chua, J.C. Ho, S.K. Chou. "A comparative study of different control strategies for indoor air humidity" *Energy and Buildings 39*, pp. 537-545, 2007.
- [26] R.T. Tamblyn. "Beating the blahs for VAV", *ASHRAE Journal Sept*, pp. 42-45, 1983.
- [27] A. Shaw. "Air conditioning control system for variable evaporator temperature." United States Patent US6269650, 2001.
- [28] K.I. Krakow, S. Lin, Z.S. Zeng. "Temperature and humidity control during cooling and dehumidifying by compressor and evaporator fan speed variation", *ASHRAE Trans 101(1)*, pp. 292-304, 1995.

- [29] M.A. Andrade, C.W. Bullard, S. Hancock, M. Lubliner. "Modulating blower and compressor capacities for efficient comfort control", *ASHRAE Trans* 108(1), pp. 631–637, 2002.
- [30] Z. Li, S.M. Deng. "An experimental study on the inherent operational characteristics of a direct expansion (DX) air conditioning (A/C) unit", *Building and Environment* 42, pp. 1–10, 2007
- [31] N. Churi, L.E.K. Achenie. "The Optimal Design of Refrigerant Mixtures for a Two-Evaporator Refrigeration System." *Computers in Chem Engng*, Vol. 21, Suppl., pp. S349-S354, 1997
- [32] W.F. Stoecker, J.W. Jones. *Refrigeration & Air Conditioning*. McGraw-Hill, Singapore, 1982.
- [33] A. Lorenz, K. Meutzner. "On application of nonazeotropic two-component refrigerants in domestic refrigerators and home freezers", in: Proc. of the XIV Int. Congress on Refrigeration, Moscow, vol.2, IIR, Paris, 1975.
- [34] R.J. Rose, D.S. Jung, R. Radermacher. "Testing of domestic two-evaporator refrigerators with zeotropic refrigerant mixtures." *ASHRAE Trans.* 98, pp. 216–226, 1992.
- [35] D.S. Jung, R. Radermacher. "Performance simulation of a two-evaporator refrigerator–freezer charged with pure and mixed refrigerants." *International Journal of Refrigerant*, Vol 14, pp. 254–263, 1991.
- [36] K.E. Simmons, K. Kim, R. Radermacher. "Experimental study of independent temperature control of refrigerator compartments in a modified Lorenz–Meutzner cycle." *ASME AES* 34, pp. 67–73, 1995.
- [37] K.E. Simmons, I. Haider, R. Radermacher, "Independent compartment temperature control of Lorenz–Meutzner and modified Lorenz–Meutzner cycle refrigerators", *ASHRAE Trans.* 102 (1), pp. 1085–1092, 1996.



- [38] H. Jiang, V. Aute, R. Radermacher. "CoilDesigner: a general-purpose simulation and design tool for air-to-refrigerant heat exchangers." *International Journal of Refrigeration*, Vol 29, pp. 601-610, 2006.
- [39] D. Richardson, H. Jiang, D. Lindsay, R. Radermacher. "Optimization of vapor compression systems via simulation." In *The International Compressor Engineering Conference and Refrigeration and Air-Conditioning Conference*, Purdue, Paper 529, 2002.
- [40] ASHRAE. "Handbook—Fundamentals", American Society of Heating, Refrigeration and Air-conditioning Engineers, Atlanta, GA, USA, 2009.
- [41] ASHRAE. "Standard 41.2 Standard Methods for Laboratory Airflow Measurement.", Atlanta, GA, USA, 1987.
- [42] ASHRAE. "Standard 37 Methods of Testing for Rating Electrically Driven Unitary Air-Conditioning and Heat Pump Equipment." Atlanta, GA, USA, 2005.
- [43] S.J. Kline, F.A. McClintok. "Describing uncertainties in single-sample experiments", *Mech Eng*, vol. 75, pp. 3-8, 1953.
- [44] L. Jia, X.F. Qian, Y.F. Wang, G. Shu. "Uncertainty analysis of air-conditioner cooling capacity measurement with air enthalpy test method", *Refrigeration and Air-Conditioning*, China Academic Journal Electronic Publishing Home, 2007.
- [45] K.F. Chan, W.M. Chin, V.R. Raghavan. "Study on a wickless heat pipe for humidity control." In *Proceedings of the 9<sup>th</sup> International Heat Pipe Symposium*, Kuala Lumpur, pp. 307-311, 2008

## LIST OF PUBLICATIONS

### Conference paper

- [1] Chan K.F., Raghavan V. R. and Chin W.M. "Study on a Two-Evaporator System for Humidity Control" The 4th International Meeting of Advances in Thermofluids, Melaka, 3-4 October 2011, pp. 1109-1117, indexed by SCOPUS and ISI, to be published by American Institute of Physics.

### Journal paper

- [1] Chan K.F., Chin W.M. and Raghavan V. R. "Feasibility Study on a Two-Evaporator System for Control of Thermal Comfort", Energy Conversion and Management (under review).

## APPENDIX A

### CHARGE OPTIMIZING TEST DATA

|                                  |                    |         |         |         |         |         |
|----------------------------------|--------------------|---------|---------|---------|---------|---------|
| Test Mode                        |                    | COOL    | COOL    | COOL    | COOL    | COOL    |
| Test Condition                   |                    | STD ISO | STD ISO | STD ISO | STD ISO | STD ISO |
| Refrigerant                      |                    | R410A   | R410A   | R410A   | R410A   | R410A   |
| Charge                           | kg                 | 2.7     | 2.8     | 2.9     | 3.0     | 3.1     |
| Thermocouple Readings            |                    |         |         |         |         |         |
| Temperature ID Air Enter DB      | ° C                | 27.02   | 27.12   | 27.09   | 27.16   | 27.04   |
| Temperature ID Air Enter WB      | ° C                | 19.03   | 19.03   | 18.94   | 18.96   | 18.96   |
| Temperature ID Air Leave DB      | ° C                | 15.69   | 15.53   | 15.37   | 15.32   | 15.17   |
| Temperature ID Air Leave WB      | ° C                | 13.86   | 13.70   | 13.52   | 13.45   | 13.36   |
| Temperature OD Air Enter DB      | ° C                | 35.07   | 35.13   | 35.22   | 35.16   | 35.15   |
| Temperature OD Air Enter WB      | ° C                | 23.91   | 23.67   | 23.72   | 23.60   | 23.88   |
| OD Air Enter Relative Humidity   | %                  | 36.12   | 35.27   | 35.26   | 34.45   | 35.96   |
| Custom Readings (Temperatures)   |                    |         |         |         |         |         |
| Temp Evaporator In After EXV     | ° C                | 16.60   | 16.20   | 15.90   | 15.70   | 15.60   |
| Temp Heat In                     | ° C                | 26.60   | 26.70   | 26.60   | 26.70   | 26.70   |
| Temp Heat Out                    | ° C                | 26.30   | 26.30   | 26.30   | 26.40   | 26.20   |
| System Readings                  |                    |         |         |         |         |         |
| Pressure Compressor Suction      | MPa                | 0.967   | 0.960   | 0.953   | 0.954   | 0.951   |
| Temperature Compressor Suction   | ° C                | 11.30   | 10.70   | 10.50   | 9.60    | 9.20    |
| Pressure Compressor Discharge    | MPa                | 2.797   | 2.813   | 2.828   | 2.848   | 2.856   |
| Temperature Compressor Discharge | ° C                | 74.90   | 75.30   | 75.60   | 75.20   | 75.10   |
| Pressure Evaporator Main In      | MPa                | 2.624   | 2.663   | 2.692   | 2.724   | 2.744   |
| Temp Evaporator Main In          | ° C                | 42.70   | 43.30   | 43.70   | 44.20   | 44.50   |
| Pressure Evaporator Main Out     | MPa                | 1.015   | 1.006   | 0.999   | 0.999   | 0.996   |
| Temperature Evaporator Main Out  | ° C                | 9.00    | 8.70    | 8.40    | 8.30    | 8.30    |
| Pressure Condenser Main In       | MPa                | 2.795   | 2.815   | 2.831   | 2.850   | 2.860   |
| Temperature Condenser Main In    | ° C                | 72.80   | 73.50   | 73.70   | 73.30   | 73.30   |
| Pressure Condenser Main Out      | MPa                | 2.734   | 2.754   | 2.773   | 2.794   | 2.805   |
| Temperature Condenser Main Out   | ° C                | 44.80   | 45.00   | 45.30   | 45.50   | 45.60   |
| Air Flow Results                 |                    |         |         |         |         |         |
| Air Flow Rate                    | m <sup>3</sup> /hr | 2637    | 2635    | 2656    | 2666    | 2660    |
| Standard Air Flow Rate           | m <sup>3</sup> /hr | 2635    | 2632    | 2653    | 2663    | 2659    |
| Custom Readings ( Others )       |                    |         |         |         |         |         |
| PRESS HEAT IN (EXV)              | MPa                | 1.158   | 1.152   | 1.148   | 1.154   | 1.154   |
| PRESS HEAT OUT (CHECK VALVE)     | MPa                | 1.158   | 1.153   | 1.148   | 1.154   | 1.154   |
| PRESS EVAPORATOR IN (EXV)        | MPa                | 1.261   | 1.249   | 1.236   | 1.228   | 1.225   |
| Performance                      |                    |         |         |         |         |         |
| Entering Air Enthalpy            | kJ/kg              | 54.442  | 54.476  | 54.202  | 54.279  | 54.27   |
| Leaving Air Enthalpy             | kJ/kg              | 39.236  | 38.83   | 38.364  | 38.185  | 37.938  |
| Sensible Heat Removal            | kW                 | 10.10   | 10.32   | 10.52   | 10.66   | 10.67   |
| Latent Heat Removal              | kW                 | 3.15    | 3.30    | 3.38    | 3.51    | 3.69    |
| Total Capacity                   | kW                 | 13.24   | 13.61   | 13.89   | 14.17   | 14.36   |
| SHF                              |                    | 0.76    | 0.76    | 0.76    | 0.75    | 0.74    |
| Total Power Input                | kW                 | 4.94    | 4.98    | 5.01    | 5.03    | 5.04    |
| COP                              | W/W                | 2.68    | 2.73    | 2.77    | 2.82    | 2.85    |
| Superheat/Sub-Cooling Results    |                    |         |         |         |         |         |
| Superheat Suction                | ° C                | 5.16    | 4.82    | 4.86    | 3.94    | 3.63    |
| Superheat Evaporator             | ° C                | 1.27    | 1.27    | 1.2     | 1.1     | 1.22    |
| Superheat Discharge              | ° C                | 28.83   | 28.98   | 29.07   | 28.35   | 28.13   |
| Subcooling                       | ° C                | 0.19    | 0.3     | 0.29    | 0.41    | 0.48    |

|                                     |                    |         |         |         |         |         |
|-------------------------------------|--------------------|---------|---------|---------|---------|---------|
| Test Mode                           |                    | COOL    | COOL    | COOL    | COOL    | COOL    |
| Test Condition                      |                    | STD ISO | STD ISO | STD ISO | STD ISO | STD ISO |
| Refrigerant                         |                    | R410A   | R410A   | R410A   | R410A   | R410A   |
| Charge                              | kg                 | 3.2     | 3.3     | 3.4     | 3.4     | 3.5     |
| Thermocouple Readings               |                    |         |         |         |         |         |
| Temperature ID Air Enter DB         | °C                 | 27.02   | 27.00   | 26.91   | 26.95   | 27.05   |
| Temperature ID Air Enter WB         | °C                 | 18.92   | 19.09   | 19.03   | 19.03   | 18.97   |
| Temperature ID Air Leave DB         | °C                 | 15.16   | 15.27   | 15.20   | 15.22   | 15.14   |
| Temperature ID Air Leave WB         | °C                 | 13.34   | 13.49   | 13.42   | 13.40   | 13.31   |
| Temperature OD Air Enter DB         | °C                 | 35.15   | 35.08   | 35.09   | 35.11   | 35.13   |
| Temperature OD Air Enter WB         | °C                 | 24.98   | 24.51   | 25.79   | 25.63   | 25.12   |
| OD Air Enter Relative Humidity      | %                  | 41.21   | 39.65   | 46.15   | 45.01   | 42.48   |
| Custom Readings (Temperatures)      |                    |         |         |         |         |         |
| Temperature Evaporator In After EXV | °C                 | 15.30   | 15.70   | 15.80   | 14.60   | 14.20   |
| Temperature Heat In                 | °C                 | 26.50   | 26.60   | 26.50   | 26.50   | 26.50   |
| Temperature Heat Out                | °C                 | 26.10   | 13.80   | 14.20   | 14.20   | 13.90   |
| System Readings                     |                    |         |         |         |         |         |
| Pressure Compressor Suction         | MPa                | 0.943   | 0.949   | 0.954   | 0.931   | 0.927   |
| Temperature Compressor Suction      | °C                 | 10.50   | 10.10   | 8.90    | 13.30   | 13.00   |
| Pressure Compressor Discharge       | MPa                | 2.852   | 2.843   | 2.850   | 2.833   | 2.852   |
| Temperature Compressor Discharge    | °C                 | 76.60   | 75.70   | 75.30   | 80.20   | 80.30   |
| Pressure Evaporator Main In         | MPa                | 2.745   | 2.725   | 2.732   | 2.741   | 2.768   |
| Temperature Evaporator Main In      | °C                 | 44.60   | 44.20   | 44.40   | 44.50   | 44.70   |
| Pressure Evaporator Main Out        | MPa                | 0.989   | 0.994   | 1.000   | 0.976   | 0.971   |
| Temperature Evaporator Main Out     | °C                 | 8.10    | 8.20    | 8.30    | 9.90    | 8.70    |
| Pressure Condenser Main In          | MPa                | 2.854   | 2.845   | 2.851   | 2.843   | 2.863   |
| Temperature Condenser Main In       | °C                 | 74.60   | 73.80   | 72.60   | 78.30   | 78.30   |
| Pressure Condenser Main Out         | MPa                | 2.799   | 2.790   | 2.794   | 2.788   | 2.807   |
| Temperature Condenser Main Out      | °C                 | 45.30   | 45.40   | 45.50   | 45.10   | 44.90   |
| Air Flow Results                    |                    |         |         |         |         |         |
| Air Flow Rate                       | m <sup>3</sup> /hr | 2686    | 2667    | 2649    | 2655    | 2644    |
| Standard Air Flow Rate              | m <sup>3</sup> /hr | 2694    | 2678    | 2653    | 2659    | 2648    |
| Custom Readings ( Others )          |                    |         |         |         |         |         |
| PRESS HEAT IN (EXV)                 | MPa                | 1.151   | 1.167   | 1.175   | 1.182   | 1.178   |
| PRESS HEAT OUT (CHECK VALVE)        | MPa                | 1.151   | 1.167   | 1.176   | 1.182   | 1.178   |
| PRESS EVAPORATOR IN (EXV)           | MPa                | 1.211   | 1.226   | 1.229   | 1.189   | 1.158   |
| Performance                         |                    |         |         |         |         |         |
| Entering Air Enthalpy               | kJ/kg              | 54.005  | 54.532  | 54.421  | 54.445  | 54.254  |
| Leaving Air Enthalpy                | kJ/kg              | 37.793  | 38.167  | 38.039  | 38.002  | 37.771  |
| Sensible Heat Removal               | kW                 | 10.80   | 10.62   | 10.51   | 10.55   | 10.66   |
| Latent Heat Removal                 | kW                 | 3.64    | 3.87    | 3.87    | 3.91    | 3.77    |
| Total Capacity                      | kW                 | 14.44   | 14.49   | 14.37   | 14.46   | 14.43   |
| SHF                                 |                    | 0.75    | 0.73    | 0.73    | 0.73    | 0.74    |
| Total Power Input                   | kW                 | 5.05    | 5.02    | 5.02    | 5.00    | 5.03    |
| COP                                 | W/W                | 2.86    | 2.88    | 2.86    | 2.89    | 2.87    |
| Superheat/Sub-Cooling Results       |                    |         |         |         |         |         |
| Superheat Suction                   | °C                 | 5.18    | 4.59    | 3.23    | 8.42    | 8.27    |
| Superheat Evaporator                | °C                 | 1.23    | 1.17    | 1.07    | 3.48    | 2.45    |
| Superheat Discharge                 | °C                 | 29.69   | 28.92   | 28.43   | 33.58   | 33.39   |
| Subcooling                          | °C                 | 0.69    | 0.45    | 0.42    | 0.71    | 1.21    |

| Test Mode                           |       | COOL    | COOL    | COOL    | COOL    | COOL    |
|-------------------------------------|-------|---------|---------|---------|---------|---------|
| Test Condition                      |       | STD ISO | STD ISO | STD ISO | STD ISO | STD ISO |
| Refrigerant                         |       | R410A   | R410A   | R410A   | R410A   | R410A   |
| Charge                              | kg    | 3.6     | 3.7     | 3.8     | 3.9     | 4.0     |
| Thermocouple Readings               |       |         |         |         |         |         |
| Temperature ID Air Enter DB         | ° C   | 27.04   | 26.94   | 26.95   | 27.03   | 27.05   |
| Temperature ID Air Enter WB         | ° C   | 18.90   | 19.09   | 19.11   | 18.86   | 18.83   |
| Temperature ID Air Leave DB         | ° C   | 14.88   | 15.00   | 15.05   | 14.78   | 14.74   |
| Temperature ID Air Leave WB         | ° C   | 13.14   | 13.30   | 13.35   | 13.00   | 12.96   |
| Temperature OD Air Enter DB         | ° C   | 35.04   | 35.07   | 35.00   | 35.01   | 34.95   |
| Temperature OD Air Enter WB         | ° C   | 23.36   | 25.37   | 24.98   | 24.29   | 23.10   |
| OD Air Enter Relative Humidity      | %     | 36.05   | 36.56   | 42.79   | 38.77   | 33.67   |
| Custom Readings (Temperatures)      |       |         |         |         |         |         |
| Temperature Evaporator In After EXV | ° C   | 13.60   | 13.60   | 13.90   | 14.00   | 13.80   |
| Temperature Heat In                 | ° C   | 26.30   | 26.10   | 26.20   | 26.20   | 26.10   |
| Temperature Heat Out                | ° C   | 25.80   | 13.70   | 14.30   | 14.10   | 13.70   |
| System Readings                     |       |         |         |         |         |         |
| Pressure Compressor Suction         | MPa   | 0.917   | 0.931   | 0.929   | 0.928   | 0.927   |
| Temperature Compressor Suction      | ° C   | 12.80   | 11.20   | 12.10   | 10.30   | 10.00   |
| Pressure Compressor Discharge       | MPa   | 2.892   | 2.889   | 2.898   | 2.902   | 2.908   |
| Temperature Compressor Discharge    | ° C   | 81.70   | 80.20   | 82.00   | 79.80   | 79.70   |
| Pressure Evaporator Main In         | MPa   | 2.807   | 2.800   | 2.812   | 2.813   | 2.818   |
| Temperature Evaporator Main In      | ° C   | 41.90   | 42.60   | 41.70   | 41.90   | 41.20   |
| Pressure Evaporator Main Out        | MPa   | 0.959   | 0.974   | 0.971   | 0.971   | 0.969   |
| Temperature Evaporator Main Out     | ° C   | 8.90    | 7.80    | 8.40    | 7.70    | 7.60    |
| Pressure Condenser Main In          | MPa   | 2.903   | 2.899   | 2.909   | 2.910   | 2.916   |
| Temperature Condenser Main In       | ° C   | 79.30   | 77.90   | 79.60   | 77.50   | 77.30   |
| Pressure Condenser Main Out         | MPa   | 2.849   | 2.843   | 2.854   | 2.857   | 2.863   |
| Temperature Condenser Main Out      | ° C   | 42.30   | 43.00   | 42.30   | 42.30   | 41.70   |
| Air Flow Results                    |       |         |         |         |         |         |
| Air Flow Rate                       | m³/hr | 2636    | 2615    | 2646    | 2649    | 2632    |
| Standard Air Flow Rate              | m³/hr | 2646    | 2623    | 2649    | 2654    | 2640    |
| Custom Readings ( Others )          |       |         |         |         |         |         |
| PRESS HEAT IN (EXV)                 | MPa   | 1.128   | 1.164   | 1.169   | 1.165   | 1.159   |
| PRESS HEAT OUT (CHECK VALVE)        | MPa   | 1.129   | 1.164   | 1.169   | 1.165   | 1.159   |
| PRESS EVAPORATOR IN (EXV)           | MPa   | 1.156   | 1.178   | 1.165   | 1.168   | 1.165   |
| Performance                         |       |         |         |         |         |         |
| Entering Air Enthalpy               | kJ/kg | 53.962  | 54.595  | 54.711  | 53.915  | 53.791  |
| Leaving Air Enthalpy                | kJ/kg | 37.283  | 37.706  | 37.872  | 36.971  | 36.85   |
| Sensible Heat Removal               | kW    | 10.88   | 10.59   | 10.66   | 10.99   | 10.98   |
| Latent Heat Removal                 | kW    | 3.72    | 4.06    | 4.09    | 3.88    | 3.80    |
| Total Capacity                      | kW    | 14.59   | 14.65   | 14.75   | 14.87   | 14.79   |
| SHF                                 |       | 0.75    | 0.72    | 0.72    | 0.74    | 0.74    |
| Total Power Input                   | kW    | 5.10    | 5.16    | 5.18    | 5.18    | 5.18    |
| COP                                 | W/W   | 2.86    | 2.84    | 2.85    | 2.87    | 2.85    |
| Superheat/Sub-Cooling Results       |       |         |         |         |         |         |
| Superheat Suction                   | ° C   | 8.4     | 6.32    | 7.3     | 5.52    | 5.27    |
| Superheat Evaporator                | ° C   | 3.04    | 1.42    | 2.14    | 1.45    | 1.39    |
| Superheat Discharge                 | ° C   | 34.19   | 32.74   | 34.41   | 32.15   | 31.97   |
| Subcooling                          | ° C   | 4.45    | 3.65    | 4.52    | 4.57    | 5.25    |

|                                     |                    |         |         |         |         |
|-------------------------------------|--------------------|---------|---------|---------|---------|
| Test Mode                           |                    | COOL    | COOL    | COOL    | COOL    |
| Test Condition                      |                    | STD ISO | STD ISO | STD ISO | STD ISO |
| Refrigerant                         |                    | R410A   | R410A   | R410A   | R410A   |
| Charge                              | kg                 | 4.1     | 4.2     | 4.3     | 4.4     |
| Thermocouple Readings               |                    |         |         |         |         |
| Temperature ID Air Enter DB         | °C                 | 27.05   | 27.04   | 27.03   | 27.02   |
| Temperature ID Air Enter WB         | °C                 | 18.94   | 18.96   | 19.08   | 18.87   |
| Temperature ID Air Leave DB         | °C                 | 14.94   | 14.94   | 14.99   | 14.75   |
| Temperature ID Air Leave WB         | °C                 | 13.18   | 13.20   | 13.28   | 12.99   |
| Temperature OD Air Enter DB         | °C                 | 34.98   | 34.99   | 34.98   | 35.03   |
| Temperature OD Air Enter WB         | °C                 | 23.23   | 23.97   | 26.03   | 25.56   |
| OD Air Enter Relative Humidity      | %                  | 34.29   | 37.65   | 47.35   | 42.10   |
| Custom Readings (Temperatures)      |                    |         |         |         |         |
| Temperature Evaporator In After EXV | °C                 | 12.60   | 12.80   | 12.80   | 12.60   |
| Temperature Heat In                 | °C                 | 26.20   | 26.10   | 26.10   | 25.90   |
| Temperature Heat Out                | °C                 | 14.20   | 14.20   | 14.50   | 14.30   |
| System Readings                     |                    |         |         |         |         |
| Pressure Compressor Suction         | MPa                | 0.904   | 0.911   | 0.916   | 0.913   |
| Temperature Compressor Suction      | °C                 | 14.10   | 13.60   | 13.50   | 12.60   |
| Pressure Compressor Discharge       | MPa                | 2.909   | 2.929   | 2.956   | 2.972   |
| Temperature Compressor Discharge    | °C                 | 85.40   | 85.50   | 85.50   | 85.10   |
| Pressure Evaporator Main In         | MPa                | 2.830   | 2.849   | 2.876   | 2.892   |
| Temperature Evaporator Main In      | °C                 | 40.30   | 39.90   | 39.60   | 39.70   |
| Pressure Evaporator Main Out        | MPa                | 0.946   | 0.953   | 0.957   | 0.954   |
| Temperature Evaporator Main Out     | °C                 | 11.70   | 10.70   | 10.70   | 8.90    |
| Pressure Condenser Main In          | MPa                | 2.923   | 2.946   | 2.972   | 2.987   |
| Temperature Condenser Main In       | °C                 | 82.90   | 83.00   | 82.90   | 82.50   |
| Pressure Condenser Main Out         | MPa                | 2.870   | 2.890   | 2.918   | 2.934   |
| Temperature Condenser Main Out      | °C                 | 40.70   | 40.40   | 40.10   | 40.10   |
| Air Flow Results                    |                    |         |         |         |         |
| Air Flow Rate                       | m <sup>3</sup> /hr | 2649    | 2628    | 2631    | 2621    |
| Standard Air Flow Rate              | m <sup>3</sup> /hr | 2656    | 2637    | 2639    | 2632    |
| Custom Readings ( Others )          |                    |         |         |         |         |
| PRESS HEAT IN (EXV)                 | MPa                | 1.175   | 1.176   | 1.187   | 1.176   |
| PRESS HEAT OUT (CHECK VALVE)        | MPa                | 1.175   | 1.176   | 1.186   | 1.176   |
| PRESS EVAPORATOR IN (EXV)           | MPa                | 1.129   | 1.133   | 1.139   | 1.136   |
| Performance                         |                    |         |         |         |         |
| Entering Air Enthalpy               | kJ/kg              | 54.13   | 54.16   | 54.559  | 53.864  |
| Leaving Air Enthalpy                | kJ/kg              | 37.412  | 37.441  | 37.653  | 36.888  |
| Sensible Heat Removal               | kW                 | 10.87   | 10.79   | 10.75   | 10.92   |
| Latent Heat Removal                 | kW                 | 3.81    | 3.79    | 4.01    | 3.86    |
| Total Capacity                      | kW                 | 14.68   | 14.58   | 14.75   | 14.78   |
| SHF                                 |                    | 0.74    | 0.74    | 0.73    | 0.74    |
| Total Power Input                   | kW                 | 5.20    | 5.24    | 5.28    | 5.30    |
| COP                                 | W/W                | 2.82    | 2.78    | 2.79    | 2.79    |
| Superheat/Sub-Cooling Results       |                    |         |         |         |         |
| Superheat Suction                   | °C                 | 10.17   | 9.42    | 9.15    | 8.35    |
| Superheat Evaporator                | °C                 | 6.29    | 5.05    | 4.91    | 3.23    |
| Superheat Discharge                 | °C                 | 37.65   | 37.45   | 37.05   | 36.42   |
| Subcooling                          | °C                 | 6.36    | 6.97    | 7.68    | 7.91    |

APPENDIX B

VAPCYC BALANCING FOR YCC60C VS YSL61C

| Component:                          |                | Evaporator-1 |
|-------------------------------------|----------------|--------------|
| <b>Inlet/Outlet Conditions</b>      |                |              |
| Port 1 Enthalpy                     | kJ/kg          | 276.3        |
| Port 1 Pressure                     | MPa            | 1.152        |
| Port 1 Temperature                  | K              | 285.11       |
| Port 1 Sat. Delta                   | K              | 0.00         |
| Port 1 Quality                      | -              | 0.274        |
| Port 1 Massflow Rate                | kg/s           | 0.099        |
| Port 2 Enthalpy                     | kJ/kg          | 432.1        |
| Port 2 Pressure                     | MPa            | 0.9493       |
| Port 2 Temperature                  | K              | 285.71       |
| Port 2 Sat. Delta                   | K              | 7.00         |
| Port 2 Quality                      | ---            | 1.04         |
| Port 2 Massflow Rate                | kg/s           | 0.099        |
| Charge                              | kg             | 0.12         |
| Percent Charge                      | %              | 0.05         |
| <b>Performance Variables</b>        |                |              |
| Heat Out                            | kW             | -15.47       |
| Work Out                            | kW             | 0.00         |
| Power Consumption                   | kW             | 0.00         |
| Component Cost                      |                | 35.26        |
| <b>Component Inputs</b>             |                |              |
| Tube Length                         | m              | 1.35         |
| Tube Vertical Spacing               | m              | 0.02         |
| Bank Horizontal Spacing             | m              | 0.01         |
| Fins Per Inch                       | 1/in           | 20.00        |
| Average Air Velocity                | m/s            | 1.68         |
| Average Air Inlet Temperature       | K              | 300.15       |
| Average Air Inlet RH                | %              | 47.00        |
| <b>Component Output</b>             |                |              |
| Simple Cost                         | \$             | 35.26        |
| Sensible Heat Load                  | kW             | 12.71        |
| Latent Heat Load                    | kW             | 2.677        |
| Sensible Heat Ratio                 | -              | 0.83         |
| Avg. Air Outlet Temperature         | K              | 286.06       |
| Avg. Air Outlet Wetbulb Temperature | K              | 286.03       |
| Avg. Air Outlet RH                  | %              | 99.73        |
| Air Side Pressure Drop              | Pa             | 54.22        |
| Saturation Temperature DP           | K              | 6.48         |
| Ref. Side Pressure Drop             | MPa            | 0.20         |
| Total Material Volume               | m <sup>3</sup> | 0.00         |
| HX Face Area                        | m <sup>2</sup> | 0.45         |
| HX Condensate                       | kg/s           | 0.00         |

APPENDIX C

REHEAT COIL TEST DATA

| Test Mode                             |       | COOL      | COOL    | COOL    | COOL    |
|---------------------------------------|-------|-----------|---------|---------|---------|
| Test Condition                        |       | STD ISO   | STD ISO | STD ISO | STD ISO |
| Refrigerant                           |       | R410A     | R410A   | R410A   | R410A   |
| Charge                                | kg    | 3.9       | 3.9     | 3.9     | 3.9     |
| <b>Thermocouple Readings</b>          |       |           |         |         |         |
| Temperature ID Air Enter DB           | °C    | 27.08     | 27.01   | 27.08   | 27.08   |
| Temperature ID Air Enter WB           | °C    | 19.16     | 18.90   | 18.97   | 18.99   |
| Temperature ID Air Leave DB           | °C    | 15.02     | 16.80   | 18.19   | 18.46   |
| Temperature ID Air Leave WB           | °C    | 13.30     | 13.45   | 13.73   | 13.82   |
| Temperature OD Air Enter DB           | °C    | 35.11     | 35.09   | 35.00   | 35.11   |
| Temperature OD Air Enter WB           | °C    | 26.18     | 24.37   | 23.59   | 24.41   |
| OD Air Enter Relative Humidity        | %     | 47.74     | 42.98   | 36.15   | 40.00   |
| <b>Custom Readings (Temperatures)</b> |       |           |         |         |         |
| Temperature Evaporator In After EXV   | °C    | 13.50     | 11.60   | 8.53    | 8.34    |
| Temperature Heat In                   | °C    | No Reheat | 21.00   | 33.80   | 42.99   |
| Temperature Heat Out                  | °C    | No Reheat | 17.10   | 16.80   | 16.89   |
| <b>System Readings</b>                |       |           |         |         |         |
| Pressure Compressor Suction           | MPa   | 0.93      | 0.90    | 0.87    | 0.86    |
| Temperature Compressor Suction        | °C    | 12.60     | 11.40   | 13.07   | 13.59   |
| Pressure Compressor Discharge         | MPa   | 2.99      | 2.90    | 2.77    | 2.77    |
| Temperature Compressor Discharge      | °C    | 84.60     | 85.13   | 85.67   | 85.79   |
| Pressure Evaporator Main In           | MPa   | 2.90      | 2.82    | 2.70    | 2.69    |
| Temperature Evaporator Main In        | °C    | 39.87     | 40.73   | 44.03   | 43.74   |
| Pressure Evaporator Main Out          | MPa   | 0.97      | 0.94    | 0.91    | 0.90    |
| Temperature Evaporator Main Out       | °C    | 8.37      | 7.20    | 9.90    | 10.50   |
| Pressure Condenser Main In            | MPa   | 3.00      | 2.92    | 2.79    | 2.79    |
| Temperature Condenser Main In         | °C    | 82.07     | 82.40   | 82.90   | 83.14   |
| Pressure Condenser Main Out           | MPa   | 2.95      | 2.86    | 2.74    | 2.73    |
| Temperature Condenser Main Out        | °C    | 40.40     | 41.23   | 44.30   | 44.50   |
| <b>Air Flow Results</b>               |       |           |         |         |         |
| Air Flow Rate                         | m³/hr | 2644      | 2636    | 2607    | 2612    |
| Standard Air Flow Rate                | m³/hr | 2645      | 2632    | 2581    | 2588    |
| <b>Custom Readings ( Others )</b>     |       |           |         |         |         |
| PRESS HEAT IN (EXV)                   | MPa   | 1.13      | 1.47    | 2.09    | 2.65    |
| PRESS HEAT OUT (CHECK VALVE)          | MPa   | 1.13      | 1.32    | 2.03    | 2.61    |
| PRESS EVAPORATOR IN (EXV)             | MPa   | 1.16      | 1.08    | 1.01    | 1.00    |
| <b>Performance</b>                    |       |           |         |         |         |
| Entering Air Enthalpy                 | kJ/kg | 54.91     | 53.96   | 54.29   | 54.32   |
| Leaving Air Enthalpy                  | kJ/kg | 37.76     | 37.71   | 38.97   | 39.04   |
| Sensible Heat Removal                 | kW    | 10.79     | 9.42    | 7.75    | 7.54    |
| Latent Heat Removal                   | kW    | 4.26      | 4.44    | 5.48    | 5.55    |
| Total Capacity                        | kW    | 15.05     | 13.86   | 13.23   | 13.09   |
| SHF                                   |       | 0.72      | 0.67    | 0.59    | 0.58    |
| Total Power Input                     | kW    | 5.34      | 5.36    | 5.14    | 5.11    |
| COP                                   | W/W   | 2.82      | 2.59    | 2.57    | 2.56    |
| <b>Superheat/Sub-Cooling Results</b>  |       |           |         |         |         |
| Superheat Suction                     | °C    | 7.8       | 7.68    | 10.5    | 11.08   |
| Superheat Evaporator                  | °C    | 2.13      | 2.12    | 5.92    | 6.59    |
| Superheat Discharge                   | °C    | 35.72     | 37.5    | 39.94   | 40.15   |
| Subcooling                            | °C    | 7.79      | 5.72    | 0.72    | 0.43    |



APPENDIX D

REFRIGERANT MASS FLOW RATE AT DIFFERENT CONDITIONS

|                           |       |           |        |        |        |
|---------------------------|-------|-----------|--------|--------|--------|
| Entering Reheat Coil Temp | °C    | No Reheat | 21.0   | 33.8   | 43.0   |
| <b>Condenser Out</b>      |       |           |        |        |        |
| Temperature               | °C    | 40.4      | 41.23  | 44.3   | 44.5   |
| Pressure                  | MPa   | 2.95      | 2.86   | 2.74   | 2.73   |
| Enthalpy                  | kJ/kg | 266.44    | 268.13 | 274.40 | 274.82 |
| <b>Evaporator Out</b>     |       |           |        |        |        |
| Temperature               | °C    | 8.37      | 7.20   | 9.90   | 10.50  |
| Pressure                  | MPa   | 0.97      | 0.94   | 0.91   | 0.90   |
| Enthalpy                  | kJ/kg | 425.52    | 425.19 | 429.12 | 429.83 |
| Enthalpy Difference       | kJ/kg | 159.08    | 157.06 | 154.72 | 155.02 |
| <b>Performance</b>        |       |           |        |        |        |
| Air Side                  | kW    | 15.05     | 13.86  | 13.23  | 13.09  |
| Refrigerant Side          | kW    | 15.80     | 14.55  | 13.89  | 13.75  |
| Mass Flow Rate            | kg/hr | 357.57    | 333.56 | 323.23 | 319.31 |

APPENDIX E  
LIST OF EQUATIONS

| No    | Equation   |
|-------|--|
| 3 - 1 | $h_{\text{air}} = 1.006 \times \text{DB} + W(2501 + 1.86 \times \text{DB})$                            |
| 3 - 2 | $Q_{\text{total, air}} = \dot{m}_{\text{air}} \times (h_{\text{air, inlet}} - h_{\text{air, outlet}})$ |
| 3 - 3 | $P_{\text{comp}} = \dot{m}_{\text{ref}} \times \Delta h_{\text{comp}}$                                 |
| 3 - 4 | $\Delta h_{\text{comp}} = h_{\text{comp, outlet}} - h_{\text{comp, inlet}}$                            |
| 3 - 5 | $\text{COP} = \frac{Q_{\text{total, air}}}{P_{\text{comp}}}$   |
| 3 - 6 | $\text{COP} = \frac{Q_{\text{total, air}}}{P_{\text{total}}}$  |
| 3 - 7 | $P_{\text{total}} = P_{\text{comp}} + P_{\text{fan}}$  |
| 4 - 1 | $Q_{\text{total, air}} = Q_{\text{total, ref}} \times \eta$  |
| 4 - 2 | $Q_{\text{ref}} = \dot{m}_{\text{ref}} \times \Delta h_{\text{ref, evap}}$                             |
| 4 - 3 | $\Delta h_{\text{ref, evap}} = h_{\text{evap, outlet}} - h_{\text{evap, inlet}}$                       |